


Advanced squirrel algorithm-trained neural network for efficient spectrum sensing in cognitive radio-based air traffic control application

Geoffrey Eappen¹ | T. Shankar¹ | Rajagopal Nilavalan² 

¹ School of Electronics Engineering, Department of Communication Engineering, Vellore Institute of Technology, Vellore, Tamil Nadu, India

² Department of Electronics and Computer Engineering, Brunel University, Uxbridge, London

Correspondence

T. Shankar, School of Electronics Engineering, Department of Communication Engineering, Vellore Institute of Technology, Vellore, Tamil Nadu, India.
Email: tshankar@vit.ac.in

Abstract

In the current scenario, there is a drastic increase in air traffic. The air to ground communication plays a crucial role in the air traffic control system. There is a limited spectrum available for aircraft to establish a connection with the Air Traffic Controller (ATC). With air traffic growth, the available spectrum is getting more congested. This paper proposed an Advanced Squirrel Algorithm (ASA)-trained neural network (NN) for efficient spectrum sensing for cognitive radio-based air traffic control applications. ASA is a novel metaheuristic-based training algorithm for an NN. With the proposed algorithm, it is possible to dynamically allocate the unused spectrum for air to ground communication between aircraft and ATC. The quantitative analysis of the proposed ASA-NN-based spectrum sensing is done by comparing it with the existing metaheuristic-based NN training algorithms, namely, particle swarm optimization Gravitational Search Algorithm (PSOGSA), particle swarm optimization (PSO), gravitational search algorithm (GSA), and artificial bee colony (ABC). Simulation-based evaluation shows that the proposed ASA-NN is capable of efficiently detecting the spectrum holes with high convergence rate as compared to PSOGSA-, PSO-, GSA-, and ABC-based algorithms.

1 | INTRODUCTION

The development in the aviation sector has resulted in the tremendous growth of the wireless communication technologies governing the air traffic control. Wide range of wireless technologies are employed to assist the on-ground surveillance and navigation of airplanes while taking off, landing, and en-route. The employed wireless devices operate at different radio channels. The radio channels in Very High Frequency (VHF) and High Frequency (HF) bands are mainly used for enabling the link between air traffic control stations and aircraft. The VHF spectrum for wireless communication between the Air Traffic Controller (ATC) and aircraft has a bandwidth of 19 MHz ranging from 118 to 127 MHz [1]. The spectral spacing of each band is 25 kHz, resulting in a total of 760 radio channels. As the flight traffic is tremendously increasing year on year, so the number of aircraft tuning to a particular station is also increasing immensely. The problem arises when

the pilots of different aircraft tune the controller frequency at the same time, thus leading to frequency congestion and also the pilot may accidentally override others. This situation can lead to incorrect information delivered to the aircraft. In addition to that, different applications correspond to aircraft communication, which further leads to the congestion of radio channels, specifically in the regions of highly crowded airports. Therefore, it is important to utilize the radio spectrum available for aircraft communication.

Concerning the above discussion, the recent studies suggest that the industrial, scientific and medical bands are highly congested [2, 3]. In contrast, a significant portion of the licensed radio spectrum is vacant and is used inefficiently [2]. In the radio spectrum allocated for aircraft communication, only around 12.5% is effectively utilized [4]. In the current scenario, there exist the problem of spectrum scarcity, and at the same time, there is also the situation of inefficient spectrum utilization [5]. With the continuous increase in the air traffic over the last

This is an open access article under the terms of the [Creative Commons Attribution](https://creativecommons.org/licenses/by/4.0/) License, which permits use, distribution and reproduction in any medium, provided the original work is properly cited.

© 2021 The Authors. *IET Communications* published by John Wiley & Sons Ltd on behalf of The Institution of Engineering and Technology

decade, the air traffic management system has predicted that the air traffic will reach its peak by 2020 [6]. The high traffic would result in more congested bandwidth for data transmission between aircraft and ATC.

Moreover, the audio data transmission from aircraft to ATC is highly delay-sensitive, with the unavailability of proper bandwidth that can cause continuous intrusion to the transmission, which will further enhance the delay issue. Such a problem calls for the research work with emphasis made on the need for wireless communication technology capable of performing dynamic spectrum access and meeting the future requirements of aviation technology with high efficiency and precision [7]. The possible solution to the problem of spectrum scarcity and providing dynamic flexibility to the wireless communication technology employed for air traffic control is the cognitive radio network (CRN) [6]. A CRN can sense its surrounding radio environment and adjust accordingly [5]. The Federal Communications Commission's report in [8] has stated the use of the underutilized licensed spectrum to increase the effective utilization of the frequency spectrum. The CRN, with its ability to sense and adapt, can opportunistically access these underutilized licensed spectra without causing interference to the Primary Users (PU)/Licensed Users (the users having the license to utilize the licensed spectrum). The CRN makes this underutilized licensed spectrum also known as spectrum hole to the secondary users (SUs) for opportunistic access. The first and one of the most important working phases of a CRN is the spectrum sensing [9]. Through different spectrum sensing techniques, the SUs find the spectrum holes and proceed further with the process of a CRN as the process of spectrum sensing is extremely vital. So, a novel Advanced Squirrel Algorithm (ASA)-trained neural network (NN) is employed for efficient spectrum sensing to improve the effectiveness of the CRN. An effective CRN would result in improved spectral and bandwidth efficiency.

2 | RELATED WORKS

The detection of the spectrum holes by cognitive radio (CR) devices and utilizing it opportunistically enhances the spectral efficiency and the channel bandwidth [6]. The spectrum sensing plays the pivotal role in the detection of vacant and thus it is the essential component of CR network. Conventional spectrum sensing includes intensive techniques like the Matched Filter (MF) [10], cyclostationary detector [5], and eigenvalue-based detector [11], as well as the simple method like Energy Detector [12]. The simplest spectrum sensing approach has weak performance under low signal-to-noise ratio (SNR) and are not efficiently able to detect the spectrum holes [5, 9, 13]. The cyclostationary detector and MF are highly efficient in detecting the spectrum holes, but the cyclostationary detector requires long sensing time to have high detection probability [6]. For a fixed frame period, a longer sensing time decreases the transmission time and thus reduces the overall opportunistic throughput. The MF technique requires priori knowledge of the signal for efficient detection. In the absence of accurate information of PU, the performance of the MF degrades [5].

Another important drawback associated with the MF is that it requires dedicated receiver for each PU signal type [14].

The drawbacks associated with conventional spectrum sensing technique calls for the necessity of efficient spectrum prediction by CR network. With intelligent prediction-based spectrum sensing it is possible for CR network to reduce the sensing time and improve energy efficiency by efficient prediction of channel state, thus skipping spectrum sensing for some time [15–19]. The NN forms the base for the intelligent prediction scheme. To maintain a trade-off between spectrum sensing efficiency and its complexity, an NN-based spectrum sensing is successfully employed in [16, 20, 21]. The Conventional-NN which is based on gradient descent-based back propagation (BP) method are prone to converge to local optima [22, 23] and has slow convergence rate [24]. Studies have confirmed that metaheuristic-based optimization technique can improve the efficiency of NN [25–28]. Because of the no free lunch theorem [29], different metaheuristic optimization is suited for the different objective functions. Selecting the proper optimization technique for improving the performance of the artificial neural network (ANN) is very crucial as the entire CRN working is dependent on it. The popular swarm-based optimization scheme like particle swarm optimization (PSO), artificial bee colony (ABC) Algorithm, genetic algorithm (GA), grey wolf optimization (GWO) and ant colony algorithm (ACA) lack proper trade-off between their exploration (Global Search) and exploitation (Local Search) abilities [29,68]. The PSO lacks proper convergence ability, whereas ACA and ABC lack in exploitation [30,67]. The GA tends to get stuck to the local best solution instead of finding the global best [31]. Such problems call for an efficient optimization scheme that has a proper trade-off between its exploration and exploitation abilities, which has a good convergence rate and can overcome local optima and converge towards global best. Therefore, advanced flying squirrel search-based algorithm is implemented and employed.

The prevailing spectrum sensing studies were more focused on binary hypothesis, i.e. temporal spectrum sensing [32–34]. The works in [9, 35] have showed that temporal cooperative spectrum sensing has better performance than the temporal non-cooperative spectrum sensing. The 3D-spatial spectrum sensing is an emerging field [34,36–39] that gives better insight about real-time implementation of CR network. The work in [34] considered 3D spatial and temporal spectrum sensing using conventional energy detector and it has its limitation in low SNR values.

The 3D-spatial and temporal spectrum sensing is carried out for non-cooperative and cooperative scenario using ASA-trained ANN-based efficient spectrum prediction. The proposed technique is compared with the existing metaheuristic-based optimization technique for ANN in spectrum sensing.

The major contributions of this paper are stated as under.

- Novel ASA-based technique for the weight optimization in NN to enhance its prediction and efficiency.
- ASA-NN for efficient spectrum sensing by performing effective spectrum status prediction.

- 3D non-cooperative spectrum sensing (3D NCSS) scheme and temporal cooperative spectrum sensing scheme for air traffic control.
- National Instrument (NI) Universal Software Radio Peripheral (USRP)-based real-time implementation of the proposed technique for temporal cooperative spectrum sensing scheme.

3 | SYSTEM MODELLING

With the affordable airlines coming into the market, the air traffic is increasing with each passing year. Such increase in air traffic calls not only for infrastructural development but also requires high technical advancement in the field of wireless communication governing the air traffic system. As the flight traffic is enormously increasing, so, the number of aircraft tuning into a station is also increasing immensely. The problem arises when the pilots of different aircraft tune the controller frequency at the same time, thus leading to frequency congestion and pilot may also accidentally override others. This situation can lead to incorrect information delivered to the aircraft. To overcome such spectrum congestion problem, an efficient spectrum sensing-based CRN is proposed for air traffic control. The spectrum sensing efficiency is improved by incorporating novel metaheuristic algorithm ASA-trained NN. The Air to Ground (A/G) communication frameworks are basic for the aircraft's secure routing. In this way, the progress to the CR-based systems ought to be finished with most extreme consideration. While designing the CRN for the A/G communication it should make sure that its effect should be minimal on the existing A/G communication infrastructure. It is to be noticed that the existing A/G communication frameworks still depend on analogue transmission frameworks. In this work, an efficient spectrum sensing technique has been proposed for the effective CR-based Air Traffic control.

This paper proposes Phase I and II for the air traffic control. For Phase I, aircrafts perform the spectrum sensing with the help of ASA optimization algorithm. As ASA behaviour which employs gliding technique to find the optimal solution depicts the landing the process of the aircraft. Moreover, the seasonal constraints in the ASA is utilized and mapped for efficient spectrum sensing by the aircraft during different weather conditions. So, ASA is efficient in assisting aircraft to detect the vacant spectrum holes during the landing process.

In Phase II, the cognitive radio sensors/spectrum sensing sensors (CRs/SSs) are deployed in the ground level performs spectrum sensing aided with ASA-trained NN. The Conventional-NN technique uses gradient descent-based BP algorithm for training and has loopholes like getting stuck to local minima and large convergence time. Whereas, ASA is a squirrel-based optimization technique in which the population of squirrels moves around the search space constituted by the optimization problem in search of an optimal solution. Squirrel position varies during the process of search based on the best solution position so obtained. The ASA has excellent balance between its exploration and exploitation abilities, moreover it has fast convergence rate. So, ASA is used as the possible

alternative for optimizing the weights of NN. The ASA is employed to optimize the weights of NN and thus to minimize the error in the prediction of spectrum holes. The information obtained by CRs are transferred to the ground CR base station, which then makes the final decision on the vacant spectrum availability. The ASA-NN-based ATC has training and working phase, during the training phase network is trained using ASA and in the working phase-trained network is employed for the spectrum hole detection. The illustrative figures depicting Phase I and II is shown in Figures 1 and 2, respectively. The blocks in Figure 1 comprise of CR base station, which is responsible for making the final decision on the presence and the absence of the PUs for ground to air communication. Blocks ATC and Aircrafts resemble incoming aircraft communicating with the ATC. The working in Figure 1 is explained as: in the case of allocated frequency band congestion for data transmission between Aircraft and ATC, the CR technique is employed. For the proposed model, aircraft perform spectrum sensing and establish link to ATC via the spectrum holes, simultaneously CRs deployed in grounds perform spectrum sensing so as to find the spectrum holes for ground to air data transmission. If the allocated frequency bands are not congested then the routine data transmission is carried out in the allotted frequency spectrum.

4 | MATHEMATICAL MODELLING

The aircraft and CRs perform periodic spectrum sensing as aircraft approaches ATC. The schematic representation of the frame structure for spectrum sensing and data transmission is as shown in Figure 3. For the data transmission, orthogonal frequency division multiplexing (OFDM) scheme is employed with fast fourier transform (FFT) of length 64. Each subcarrier has the bandwidth of 10 kHz and total bandwidth of 0.5 MHz with 50 subcarriers. Each 25 subcarriers are used for air to ground and ground to air transmission.

The conventional spectrum sensing considers the binary hypothesis for the detection as in Equation (1) [6]:

$$\begin{aligned} H_0 : y_i(n) &= N_i(n) \\ \{\text{Hypothesis 0 (PU Absent)}\} \\ H_1 : y_i(n) &= x_i(n) + N_i(n) \\ \{\text{Hypothesis 1 (PU Present)}\}, \end{aligned} \quad (1)$$

where x_i is the PU signal which can be modelled as the zero mean complex Gaussian with the power σ_x^2 , N_i is the zero mean complex AWGN (additive white Gaussian noise) with the power as σ_N^2 [34], $n = 1, 2, \dots, m$, m is the total sample number.

$i = 1, 2, \dots, K$ (K is the total number of aircraft arriving at the airport at the same time). $j = 1, 2, \dots, L$ (L is the total number of SSs/SUs or cognitive radio users (CRu) operating in a cooperative manner).

According to the binary hypothesis, a spectrum sensing can accept or reject samples and infer the presence and the absence of the PU based on the detection threshold as [40]

$$E_i = \frac{1}{K} \sum_{i=1}^K |y_i(n)|^2 \underset{H_0}{\overset{H_1}{\geq}} \lambda, \text{ here } \lambda \text{ is the detection threshold.}$$

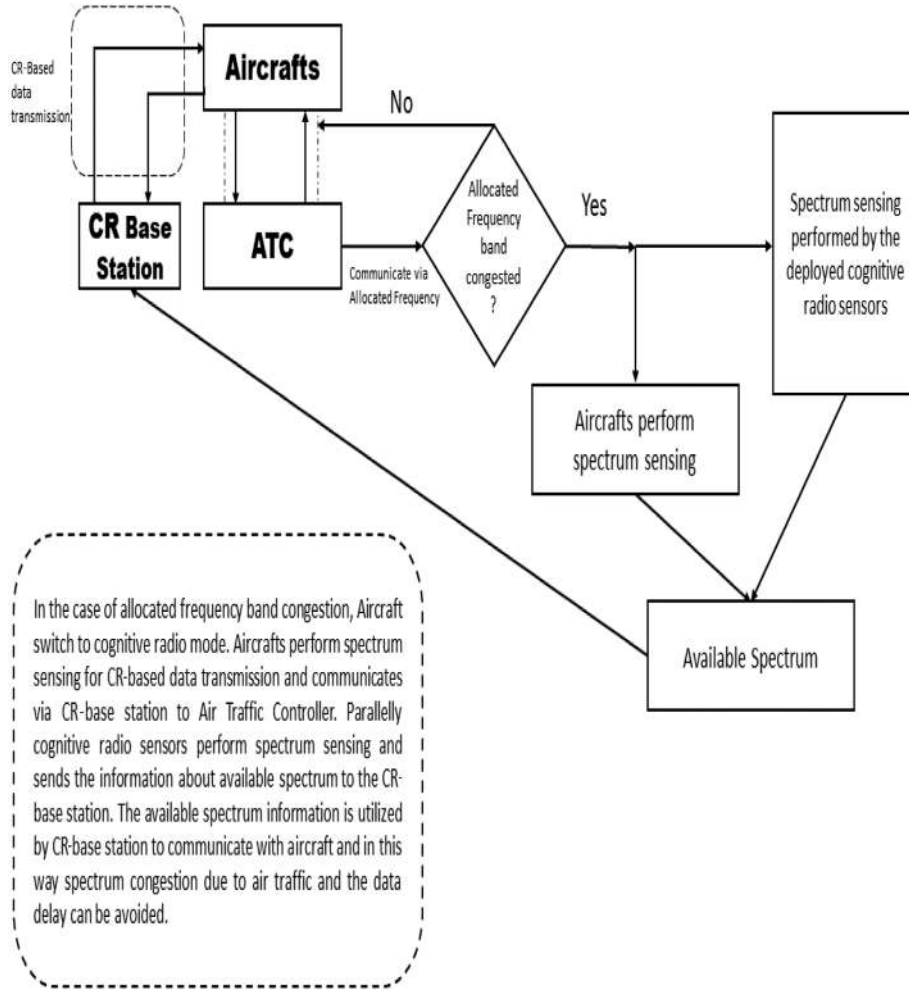


FIGURE 1 Flow diagram of the proposed CR-based ATC (Phase I)

Energy sample value greater than the threshold would be considered as the PU present and vice versa for the energy sample value lower than the threshold. The $x_i(n)$ is the n th sample sensed by the i th aircraft. Similar hypothesis can be employed for the j th SS.

The two phases of spectrum sensing is considered and is operated simultaneously for this research. The binary hypothesis holds good for the ground-based CRu performing cooperative spectrum sensing. For the aircraft to perform spectrum sensing, it is necessary that it performs spectrum sensing when it is near to ground (looking for ground clearance to land), so that it can be within the coverage area of some PU transmitter. It is because, if aircraft performs spectrum sensing outside the range of PU then there will be high false alarm. Thus, the aircraft can cause interference to the PU's transmission while performing down link data transmission to the ATC.

From Figure 4, it can be seen that $(D_0 - D_1)$ is the region in which aircraft is outside the coverage area of PU and D_1 represents the radius of PU transmission range. The hypotheses H_0 and H_1 for the aircraft approaching an ATC can be validated only when it is inside the radius D_1 . The formulation of the

spatial hypothesis can be written as in Equation (2):

$$\begin{cases} B_0 & D_1 \cap H_0 \\ B_1 & D_1 \cap H_1 \\ B_2 & D_0 \cap H_0 \\ B_3 & D_0 \cap H_1 \end{cases} \quad (2)$$

where $B_0 = D_1 \cap H_0$ represents that the aircraft is within the range of PU Transmitter–Receiver (Tx–Rx) coverage and the Hypothesis H_0 holds true (i.e. PU is inactive). Thus, aircraft have the spectrum access opportunity. The $B_1 = D_1 \cap H_1$ indicates that PU is active and aircraft is within the PU Tx–Rx coverage.

From Equations (1) and (2), the modified hypothesis can be postulated as:

$$\begin{aligned} B_0 : y_i(n) &= N_i(n) & 0 \leq d_i \leq D_1 \\ B_1 : y_i(n) &= x_i(n) + N_i(n) & 0 \leq d_i \leq D_1 \\ B_2 : y_i(n) &= N_i(n) & D_1 \leq d_i \leq D_0 \\ B_3 : y_i(n) &= N_i(n) & D_1 \leq d_i \leq D_0 \end{aligned} \quad (3)$$

The condition B_2 and B_3 cannot be employed as the spectrum opportunity for the aircraft. Only B_0 is the available spectrum

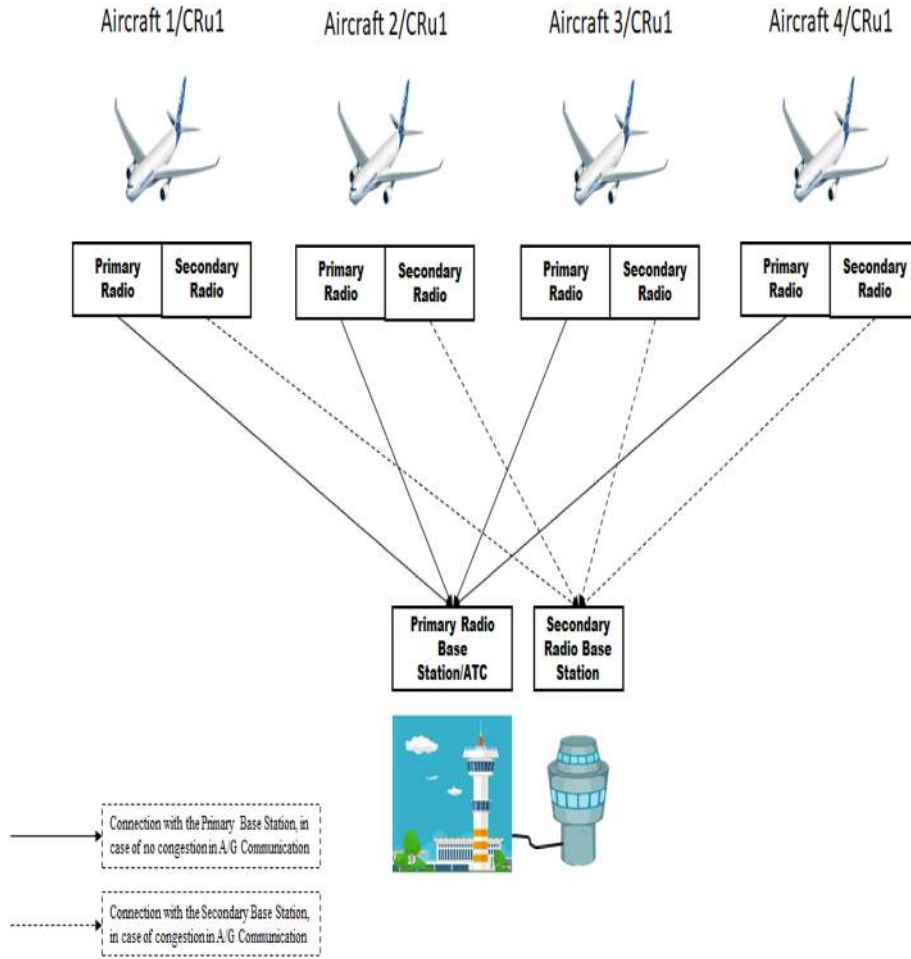


FIGURE 2 Proposed CR-based ATC (Phase II)

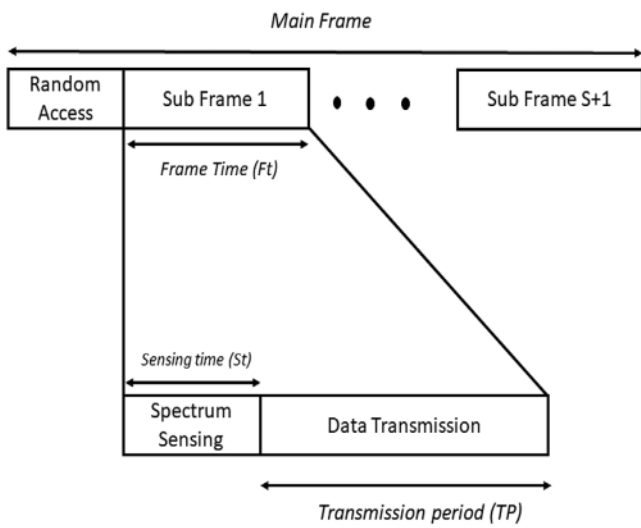


FIGURE 3 Proposed CR-based ATC (Phase II)

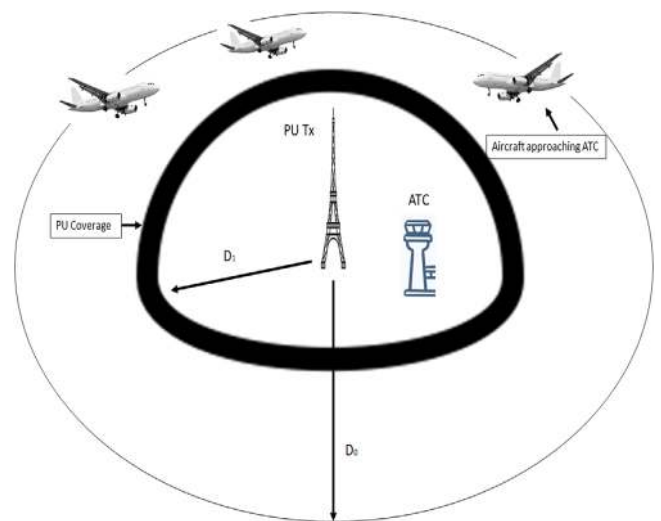


FIGURE 4 Schematic representation of PU coverage for aircraft spectrum sensing

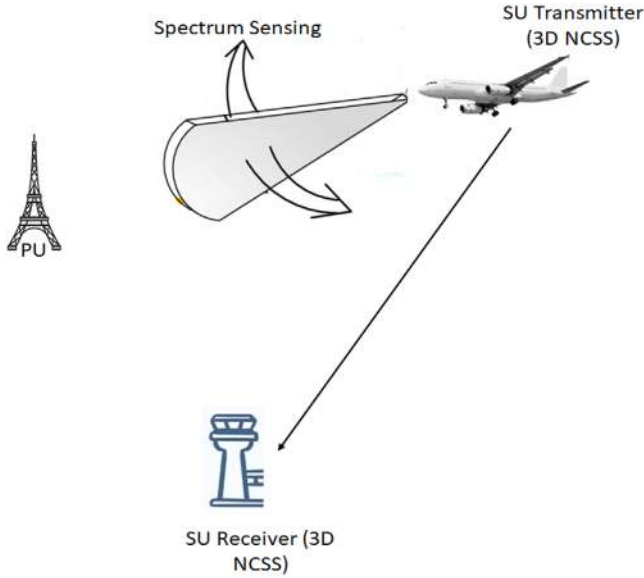


FIGURE 5 Schematic representation of spectrum sensing for the case 3D NCSS

opportunity (i.e. the Aircraft is within the PU coverage and PU is inactive).

4.1 | 3D NCSS by aircraft

The two phases of spectrum sensing is considered simultaneously. The Phase I spectrum sensing performed by the aircraft is termed as the 3D NCSS because each aircraft performs spectrum sensing without any cooperation with the other aircraft and also the spectrum sensing is performed during descent, so three-dimensional space has been considered. Figure 5 shows the schematic representation of spectrum sensing performed during the 3D NCSS scenario/Phase I.

In Phase II, the SSs are deployed in the ground near ATC performs spectrum sensing in cooperative manner (i.e. spectrum sensing data of each SUs are beamed towards the fusion centre (FC), which makes the final decision on spectrum occupancy). Therefore, Phase II is termed as the cooperative spectrum sensing scheme.

For Phase I, to evaluate the performance of spectrum sensing the probability of detection and the probability of false alarm is employed. Based on Equation (3), the probability of detection and the false alarm can be calculated as in Equation (4):

$$\begin{aligned} P_{f,i}^{Nc}(\kappa) &= P(B_1|B_0) \\ P_{d,i}^{Nc}(\kappa) &= P(B_1|B_1), \end{aligned} \quad (4)$$

where, $P_{f,i}^{Nc}(\kappa)$ is the probability of the false alarm of the i th aircraft under non-cooperative spectrum sensing scheme for the

κ th sensing period. The $P_{d,i}^{Nc}(\kappa)$ is the probability of the detection of the i th aircraft under non-cooperative spectrum sensing scheme for the κ th sensing period. For each aircraft as well as for the SSs, energy detector is employed for obtaining the energy samples while performing the spectrum sensing. In case of cooperative spectrum sensing scheme performed by the SUs, the samples are used for training the ASA-based NN at CR base station/ (FC).

The test statistics for energy detection-based spectrum sensing is written as in Equation (5):

$$e_i(\kappa) = \frac{1}{m} \sum_{n=1}^m |x_i(n)|^2. \quad (5)$$

For large number of samples, the term $e_i(\kappa)$ as per the Central Limit Theorem (CLT) can be approximated as a Gaussian random variable for the Hypotheses H_0 and H_1 of Equation (1)[12, 41].

$$e_i(\kappa) \sim \begin{cases} N\left(\sigma_N^2, \frac{\sigma_N^4}{m}\right) : H_0 \\ N\left((1 + SNR_{TV,r,i})\sigma_N^2, (1 + SNR_{TV,r,i})^2 \frac{\sigma_N^4}{m}\right) : H_1, \end{cases} \quad (6)$$

where $SNR_{TV,r,i}$ is the received SNR of the PU (TV received power) at the i th aircraft.

Based on the approximation in Equation (6), the $P_{f,i}^{Nc}(\kappa)$ and $P_{d,i}^{Nc}(\kappa)$ can be estimated as in Equations (7) and (8), respectively:

$$P_{f,i}^{Nc}(\kappa) = Q\left(\frac{\lambda - \sigma_N^2}{\frac{\sigma_N^4}{m}}\right), \quad (7)$$

$$P_{d,i}^{Nc}(\kappa) = Q\left(\frac{\lambda - (1 + SNR_{TV,r,i})\sigma_N^2}{(1 + SNR_{TV,r,i})^2 * \frac{\sigma_N^4}{m}}\right), \quad (8)$$

where λ is the detection threshold to mark the difference between the PU's presence and absence.

4.2 | Cooperative spectrum sensing by SSs/SUs/CRu

The energy detection samples from SUs are transferred to the FC. The FC with the help of ASA-NN makes the correct prediction about the vacant spectrum. The detailed working of ASA-NN-assisted spectrum hole prediction by FC is explained in Section 6. The cooperative spectrum sensing scheme employed by the SSs is explained as below: At FC, the linearly weighted energy values from all SUs are obtained as in

Equation (9):

$$e_{css} = \sum_{j=1}^L W_j e_j, \quad (9)$$

where e_j is the energy detected by the j th SU, W_j is the weight coefficient of the j th SU and it is calculated as shown in Equation (10):

$$W_j = \frac{SNR_{TV,r,j}}{\sqrt{\sum_{l=1}^L SNR_{TV,r,l}}}, \quad (10)$$

where $SNR_{TV,r,j}$ is the received SNR at the j th SU. In Equation (10), $l \neq j$ and l corresponds to other SUs. The weighted energy value e_{css} can be approximated as Gaussian random variable as in Equation (11) for the Hypotheses H_0 and H_1 in Equation (1):

$$e_{css} \sim \begin{cases} N(\mu^0, \sigma^0) \\ N(\mu^1, \sigma^1), \end{cases} \quad (11)$$

where

$$\begin{aligned} \mu^0 &= \sum_{j=1}^L W_j \sigma_n^2 \\ \sigma^0 &= \sum_{j=1}^L W_j \frac{\sigma_n^4}{m} \\ \mu^1 &= \sum_{j=1}^L W_j (1 + SNR_{TV,r,j}) \sigma_n^2 \\ \sigma^1 &= \sum_{j=1}^L W_j (1 + SNR_{TV,r,j})^2 \frac{\sigma_n^4}{m}. \end{aligned} \quad (12)$$

Using Equations (11) and (12), the probability of false alarm and the probability of detection can be calculated as Equations (13) and (14):

$$P_{f,j}^{cs}(k) = Q\left(\frac{\lambda - \mu^0}{\sigma^0}\right), \quad (13)$$

$$P_{d,j}^{cs}(k) = Q\left(\frac{\lambda - \mu^1}{\sigma^1}\right). \quad (14)$$

In general, the opportunistic throughput of the SU performing data transmission in the absence of PU can be calculated as in Equation (15)

$$T^{opt} = P^{H_0} \left(\frac{Ft - St}{Ft} \right) (1 - P_f) \log_2(1 + SNR), \quad (15)$$

where T^{opt} denotes the opportunistic throughput, Ft and St are the frame time and the sensing time, respectively. The P^{H_0} denotes the probability that PU is inactive, generic false alarm probability, and the SNR of SU (while performing oppor-

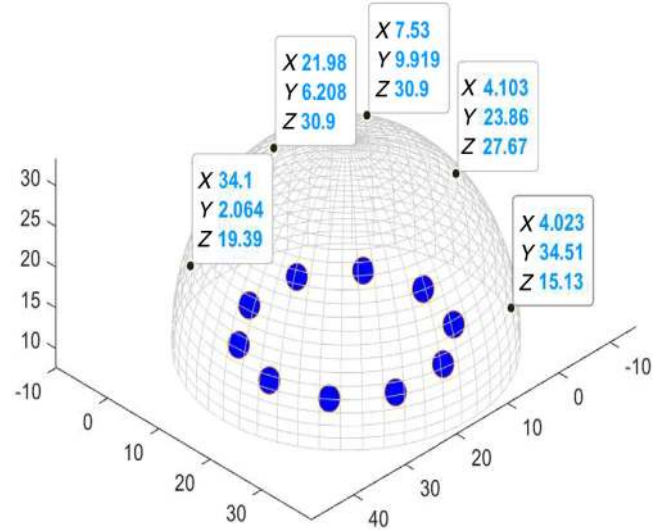


FIGURE 6 Simulation-based representation of the proposed model

tunistic data transmission) is represented as P_f and SNR , respectively.

In Figure 6, the hemispherical dome represents the PU coverage and within this coverage CRs are deployed as represented by blue circles and the approaching aircraft towards ATC is represented by black dots with coordinates.

5 | CONVENTIONAL FLYING SQUIRREL SEARCH ALGORITHM

Flying Squirrel Search Algorithm (FSSA) is introduced by Jain et al. [42] and it is based on the effectual foraging behaviour of flying squirrels. The search for the food sources depends on weather, type of trees, and the presence and the absence of the predators. The flying squirrels are more active in warm weather than cold and are capable of obtaining better and abundant food source during that period. The flying squirrels consumes two types of food sources, i.e. Hickory nuts (Hickory tree) and Acorn nuts (Acorn tree). The Acorn nuts which are abundantly available during warm weather is immediately consumed by the squirrels whereas the Hickory nuts are stored for winter. During winter flying squirrels are inactive, so it is difficult for them to obtain new foods. Therefore, storing Hickory nuts is one of the prime motives so as to withstand the extreme weather condition.

5.1 | FSSA initialization

The algorithm starts with the initialization of parameters: Maximum Iteration = it^{\max} , Size of squirrel population = M , Decision variable count/Number of dimensions = D , Probability of predator's presence = P_{rp} , Scaling factor = s^f (value ranges between 16 and 37), Gliding distance constant = G^c , and Decision variable bounds.

5.1.1 | Random initialization of flying squirrels (F_s)

For the population count ' M ' and with the upper and lower bounds as F_s^u and F_s^l , respectively, then each flying squirrels can be randomly initialized using Equation (16):

$$F_{s_{I,\zeta}} = F_{s_{\zeta}}^l + rand() \times (F_{s_{\zeta}}^u - F_{s_{\zeta}}^l), \quad (16)$$

where $F_{s_{I,\zeta}}$ represents I th flying squirrel in the ζ th dimension, $rand()$ generates random number between 0 and 1, $I = 1, 2, 3 \dots M$, and $\zeta = 1, 2, 3 \dots D$.

The fitness of a squirrel in a particular dimension represents its location and the quality of the solution. In the FSSA, optimal solution location is mapped as optimal food source (Hickory nuts) which is termed as the location of squirrel at Hickory tree. The next best solutions are termed as the location of squirrel at Acorn tree. The normal solutions (Acorn nuts) are termed as location of squirrel at normal food source, i.e. Normal tree. After random initialization of the flying squirrels, the squirrels with maximum fitness value are noted as to be on the Hickory nut tree. The next few best solutions are termed as squirrels' locations on the Acorn nut trees. The rest of the squirrels are considered to be on Normal tree. While foraging it is important to consider the probability of predator's presence (P_{rp}).

5.1.2 | Movement of flying squirrels towards new solutions

Squirrels on Acorn tree tends to move towards Hickory nut tree, i.e. the best solution found so far using Equation (17):

$$F_{s_a}^{t+1} = \begin{cases} F_{s_a}^t + d^g \times G^g \times (F_{s_b}^t - F_{s_a}^t) & r_1 \geq P_{rp} \\ \text{Random Location} & \text{otherwise,} \end{cases} \quad (17)$$

where t is the iteration number ranging from 1, 2, 3 ... it^{\max} , r_1 is the random number between [0,1]. The term d^g is the random gliding distance and its value ranges in between 9 and 20 m [42], however a large value of d^g can cause deviation in squirrel movements and can result in underperformed optimization algorithm. So, d^g is divided by a scaling factor which is a non-zero term and its value can range from 16 to 37 [42]. The gliding constant G^g helps in maintaining the trade-off between exploration and exploitation abilities of the FSSA and its value is considered as 1.9 [42]. The value of P_{rp} is taken as 0.1.

Some squirrels which are on normal food source tree will move towards better food location, i.e. (Hickory nut tree and Acorn nut tree) as per Equations (18) and (19):

Normal tree to Hickory tree:-

$$F_{s_n}^{t+1} = \begin{cases} F_{s_n}^t + d^g \times G^g \times (F_{s_b}^t - F_{s_n}^t) & r_2 \geq P_{rp} \\ \text{Random Location} & \text{otherwise} \end{cases} \quad (18)$$

Normal tree to Acorn tree:-

$$F_{s_n}^{t+1} = \begin{cases} F_{s_n}^t + d^g \times G^g \times (F_{s_a}^t - F_{s_n}^t) & r_3 \geq P_{rp} \\ \text{Random Location} & \text{otherwise,} \end{cases} \quad (19)$$

here r_1 and r_2 are random numbers between 0 and 1.

The movement of squirrel is governed by gliding aerodynamics principle [42]. The foraging behaviour of the conventional FSSA also governed by seasonal monitoring condition which maintains a proper balance between its exploration and exploitation abilities.

Imitating the behaviour of squirrel during winter season which makes the algorithm more realistic, season monitoring condition is employed in conventional FSSA. For this purpose, season constant in Equation (20) is compared with season monitoring condition in Equation (21).

Season Constant:

$$SC_t = \sqrt{\sum_{\zeta=1}^D (F_{s_{a,\zeta}}^t - F_{s_{b,\zeta}}^t)^2} \quad (20)$$

Season Monitoring Condition:

$$SM_{\min} = \frac{10E^{-6}}{(365)^t / (it^{\max} / 2.5)}. \quad (21)$$

If $SC_t \leq SM_{\min}$ then the flying squirrels are relocated using Equation (22):

$$F_s = F_s^l + Levy(n) \times (F_s^u - F_s^l). \quad (22)$$

6 | ADVANCED SQUIRREL ALGORITHM

6.1 | Motivation

As per the 'No Free Lunch Theorem' [43], the evolutionary-based optimization algorithm's performance varies based on the optimization problems. A distinct optimization algorithm is suited for distinct problems. For an optimization algorithm to have a good performance, it should start with the good exploration abilities. Towards the later stage, the search should be around the elite individual with better exploitation as compared to exploration so as to achieve a good convergence. Moreover, the algorithm should make sure that it does not get stuck to local optima. Hence, in an optimization algorithm, there should be proper trade-off between its exploration and exploitation abilities.

6.2 | Modification

The main objective with the modification in an optimization algorithm is that it should perform search around elite individual and should prevent local optima. In order to improve

the FSSA, the modifications are made to enable ASA to prevent local optima and have better trade-off between its exploration and exploitation abilities.

6.2.1 | Crossover and mutation

In conventional FSSA due to the lack of evolution, the diversity level is low and as the result the algorithm can get trapped to the local optima solution. But for a population-based algorithm in order to solve highly complex problem it is very much required to have high dimensional diversity, so as to ensure the search process searches for the global best solution [29].

The technique of crossover and mutation is incorporated to the conventional FSSA in order to obtain the optimum weight values for training the NN. The entire population is divided in two equal sub-population $F_{1s_i, \zeta}$ such that ($I = 1, \dots, M/2$ and $\zeta = 1, \dots, D$) and $F_{2s_i, \zeta}$ such that ($I = M/2, \dots, M$ and $\zeta = 1, \dots, D$).

The random initialization of the search agent/squirrels of each sub-population is performed using Equation (16). Each sub-population has its own population diversity and the algorithm proceed with finding of new solutions using Equations (17)–(19) for each sub-population separately. The best solution and its position from each sub-population, i.e. (Squirrel position at Hickory nut tree) is retrieved and stored in memory. The linear crossover is then employed to it as shown in Equation (23) and the solutions are stored in the memory.

$$F_{s_b}^{c,t} = \rho F_{s_{1b}}^t + (1 - \rho) F_{s_{2b}}^t, \quad (23)$$

here ρ is random number between 0 and 1, $F_{s_{1b}}^t, F_{s_{2b}}^t$ are the best solution from population set 1 and 2, respectively, and $F_{s_b}^{c,t}$ is the solution generated after the crossover between two best solutions from each sub-population at t th iteration. The $F_{s_b}^{c,t}$ is also stored in the memory.

Post crossover all the best solutions stored in the memory are mutated. The Gaussian Mutation is employed as shown in Equation (24).

$$\begin{aligned} F_{s_b}^{m,t} &= F_{s_b}^{c,t} + (F_s^u - F_s^l) \times ga(0, \vartheta) \\ F_{s_{1b}}^{m,t} &= F_{s_{1b}}^t + (F_s^u - F_s^l) \times ga(0, \vartheta) \\ F_{s_{2b}}^{m,t} &= F_{s_{2b}}^t + (F_s^u - F_s^l) \times ga(0, \vartheta), \end{aligned} \quad (24)$$

here $F_{s_b}^{m,t}, F_{s_{1b}}^{m,t}, F_{s_{2b}}^{m,t}$ are the mutated solutions of crossover solution and the best solutions from each sub-population, respectively. The $ga(0, \vartheta)$ is the Gaussian mutation factor with 0 mean and ϑ as the variance. In order to have emphasis on exploration and exploitation during different stages of iteration, i.e. to ensure high exploration during the start of iteration and high exploitation during later stage, the ϑ is decreased as $\vartheta(t+1) = \vartheta(t) \times e^{-t}$.

The mutated solutions stored in a repository are compared with the solutions in memory and the best solution is selected.

In this way, at the end of each iteration the best solution is retained and stored in the separate repository.

6.2.2 | Chaotic winter selection

The important factor to be considered for incorporating a modification into an optimization algorithm is its application. The ASA is employed for training the NN, i.e. weight optimization of the NN to minimize the error in the correct prediction of the spectrum holes. The conventional squirrel algorithm employs *Levy* distribution for reallocating the squirrels that could not reach to an optimal food source at the end of winter season as shown in Equation (21) [42]. This process of updating the squirrel position is meant for enhancing the exploration ability of the algorithm. The *Levy* distribution approach cannot guarantee the optimized random blind search for the sparse targets [44]. Moreover, the presence of bias can overshoot the target [44] and which is not suitable for training an NN. Hence, the sinusoidal chaotic approach is employed for relocating the squirrels at the end of winter season.

Sinusoidal chaotic approach is as shown in Equation (25) used generate random sequence as CH .

$$CH_{n+1} = Cb \cdot CH_n^2 \cdot \sin(\pi CH_n), \quad (25)$$

here $Cb = 2.3$ and the initial value of CH_0 is taken as 0.7, after modification Equation (22) can be rewritten as in Equation (26)

$$F_s = F_s^l + CH_n \times (F_s^u - F_s^l). \quad (26)$$

7 | THEORETICAL ANALYSIS OF ASA COMPARED WITH THE EXISTING ALGORITHM EMPLOYED FOR TRAINING NN

Because of the drawbacks associated with the Conventional-NN [22, 24], the efforts were made in improving the performance of NN using metaheuristic algorithms [23, 27]. The ASA is compared with the hybrid Particle Swarm Optimization Gravitational Search Algorithm (PSOGSA), PSO, Gravitational Search Algorithm (GSA), ABC Algorithm employed in training the NN. All the mentioned algorithms are used in weight and bias optimization of NN so as to have minimized error between the target and the predicted information about the presence and the absence of PU.

The PSO is based on the flocking behaviour of the swarms [45], the governing equations of PSO are :

$$X_i^{t+1} = X_i^t + V_i^{t+1}, \quad (27)$$

$$\begin{aligned} V_i^{t+1} &= WV_i^t + C_1 R_{i1} (\text{Personalbest}_i - X_i^t) \\ &+ C_2 R_{i2} (\text{Globalbest}_i - X_i^t), \end{aligned} \quad (28)$$

Equation (32):

$$O(b_c) = \frac{1}{1 + e^{-b_c}}, \quad (32)$$

where $c = 1, 2, \dots, H$ and $b_c = \sum_{g=1}^N w_{gc} X_g - b_c$, w_{gc} is the weight value between g th input node and c th hidden node. The bias connected to the c th hidden node is represented by b_c and X_g is the input from g th input node.

The hidden nodes are connected via weights and biases to the output node and the output from the output node can be represented by Equation (33):

$$O_o = \sum_{c=1}^H w_{oc} O(b_c) - b_o, \quad (33)$$

here $o = 1, 2, \dots, M$, w_{oc} is the weight connection from the c th hidden node to the o th output node, b_o is the bias connected to the o th output node.

The error e^d (fitness function) and its average value is calculated as in Equations (34) and (35):

$$e^d = \sum_{g=1}^N (A_g^d - T_g^d), \quad (34)$$

$$e = \sum_{d=1}^D \left(\frac{e^d}{D} \right), \quad (35)$$

here T_g^d = Target output corresponding to the g th input node for the d th training sample.

A_g^d = Actual output for the g th input node corresponding to the d th training sample.

The objective function for the ASA for the weight and bias optimization in NN is as Equation (36)

$$\min_{w,b} e \quad (36)$$

Figure 7 shows the NN model and Figure 8 shows a pictorial representation of ASA employed for weight optimization of an NN. During the training phase for a given training input samples, the weights are randomly initialized. The random weights are then fed to the ASA optimization as shown in Figure 8. The ASA starts with the sub-population formation and random initialization of search agents based on Equations (17)–(19) in the search space of the weight optimization to minimize the error as in Equation (35). This process of crossover, mutation, and chaotic winter selection is then employed based on Equations (23), (24), and (26), respectively, so as to obtain the optimized weight values to minimize the error. In this way, initial weight values are then optimized using ASA and fed back to the NN for the correct detection of the spectrum holes. Figure 8 comprises of CRs whose spectrum sensing samples are fed to the ASA-NN at CR base station/FC for the channel prediction.

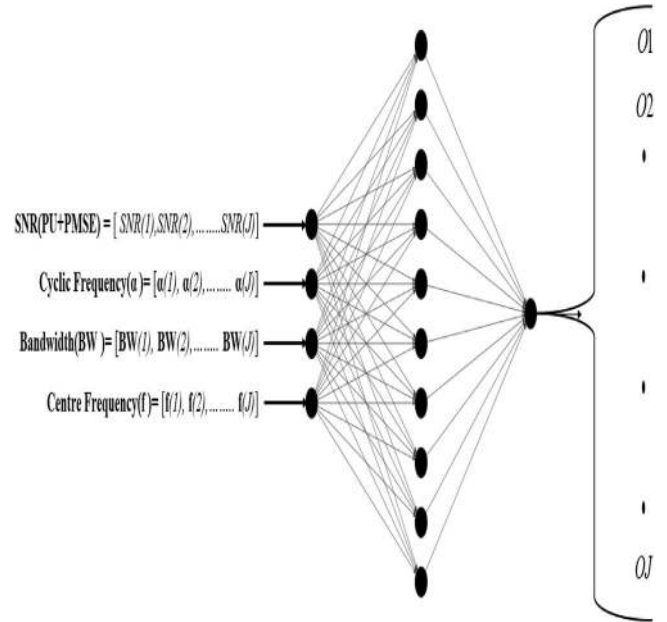


FIGURE 7 Pictorial representation of NN model employed for spectrum prediction

8.1 | ASA-NN for channel prediction

The ASA-trained NN is employed for efficient channel prediction in CR-based ATC. The PU mainly considered is the TV Broadcast system of a particular geographical location (i.e. United Kingdom). For training NN, it is required to have optimized weights, biases, and proper training input samples such that NN should be efficiently able to differentiate between PU's presence and absence from the channel state information.

In a TV band, the presence of TV signals can be identified by its centre frequency, bandwidth, and the signal power level. Moreover, TV signals employs modulations, therefore they exhibit statistical properties as a periodic function of time, i.e. the cyclostationary property [5]. For the correct prediction from the channel state, the input samples employed for training are SNR, Bandwidth of the PU, the centre frequency of the PU, and the cyclic frequency associated with each centre frequency of PU. The ASA optimizes the weights and biases of NN in the MATLAB environment using pre-defined samples with the goal of minimizing the error to 1×10^{-30} .

The proposed ASA-NN employed for channel prediction comprises of a training period and a working period. The training period will be the same for SU of the 3D non-cooperative spectrum sensing scheme and the CRs of the cooperative spectrum sensing scheme. In the working period of the 3D non-cooperative spectrum sensing scheme, SUs (Aircraft) makes the final decision on the channel state based on the knowledge base and the ASA-NN of the training period. In the case of cooperative spectrum sensing, CRs perform the spectrum sensing and the data is sent to the FC, where trained ASA-NN is employed to make final decision based on received samples

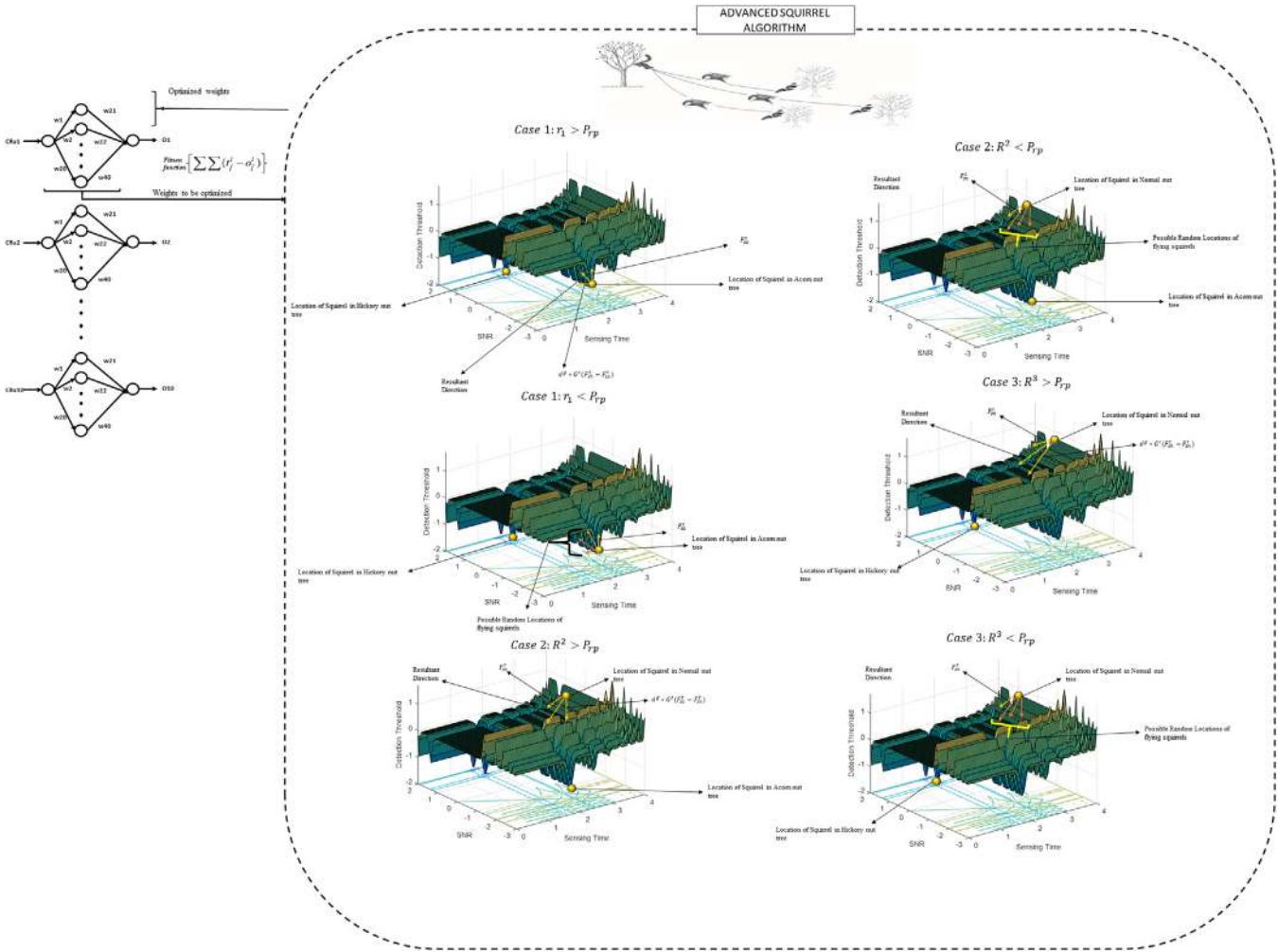


FIGURE 8 Pictorial representation of ASA-based weight optimization of NN

from CRs. In the proposed work, the real-time input samples are obtained using USRP N210 and B210, these input samples are then fed to the ASA-NN in the MATLAB environment. The ASA-NN makes the binary channel state prediction (1: PU is present, 0: PU is absent) based on the input samples. With the help of input samples and the optimized weights and bias values, the proposed ASA-NN is able to efficiently detect the spectrum holes and can enhance the opportunistic throughput of the SU. The input sample description is as follows:

1. SNR: It is considered that the TV transmitter is equipped with omnidirectional antenna and it is transmitting signal with a transmission power ranging from 10 to 50 kW [51]. As the TV transmission is assumed to have coverage up to 2.5 km, so an SU within this coverage can opportunistically utilize the spectrum to enhance its bandwidth. The TV power received within its coverage area depends on the distance between its transmitter and receiver. The relation between TV transmitted power and the received power as the function of distance can be denoted as in

Equation (37) [52].

$$TV_{(rvp)} = TV_{(trp)} \left(\frac{d'_0}{d'} \right)^{n'}, \quad (37)$$

here $TV_{(rvp)}$ is the power received at TV receiver, $TV_{(trp)}$ is the power received by TV receiver for a reference distance of d'_0 , as d'_0 is considered 10 m, so for such a small value of reference distance the $TV_{(trp)}$ is considered equal to the TV transmitter power. $n' = 3$, d' is the distance between TV transmitter and TV receiver.

With noise power spectral density as N_0 and specific bandwidth B , the SNR of the TV transmission received can be written as in Equation (38).

$$SNR_{TV_r} = \frac{TV_{(rvp)}}{BN_0}. \quad (38)$$

As the distance increases SNR_{TV_r} decreases. The Federal Communications Commission (FCC) has defined certain

TABLE 1 PMSE bandwidth and power

PMSE devices	$P_{dBm/B}^{PMSE}$	B
Wireless microphone	-78	200 kHz
In-ear monitors	-78	200 kHz
Talkback	-78	200 kHz
Data links	-78	200 kHz
Program audio links	-78	200 kHz
Program video links	-65	8 MHz

minimum threshold level for SNR_{TV_r} [51, 53, 54]. So the SNR_{TV_r} samples between its max and min bound are employed as one of the input for training ASA-based NN. The TV frequency band in U.K. 470–790 MHz (channel 21–60) in any particular location not used by digital terrestrial television (DTT) could be used by low power devices. The Programme Making and Special Events (PMSE) equipment like wireless microphone and audio devices have been using these white spaces on opportunistic manner with the assistance of white space database (WSDB). The CR devices (CRd)/ white space devices (WSD) operating in these frequency range should not only consider the presence of DTT but also the PMSE before transmission. The PMSE power can be calculated as in Equation (39) [55].

$$P_{dBm/B}^{PMSE} = P_{dB}^{SU-PMSE} + r(\Delta f)_{dB} + m_{dB}^{G1} + \gamma_{dB} + 19.03, \quad (39)$$

where $P_{dBm/B}^{PMSE}$ is the PMSE signal power over its channel bandwidth B , $P_{dB}^{SU-PMSE}$ is the power spectral density limit of the CRd signal to avoid interference with the PMSE signals, m_{dB}^{G1} is the coupling gain between CRd and PMSE signals. The coupling gain margin is denoted by γ_{dB} , $r(\Delta f)_{dB}$ is the ratio of PMSE signal power over CRd signal power at PMSE receiver. The Δf is the channel separation (DTT-8 MHz) between CRd and PMSE signal. The value 19.03 is equivalent to $10\log_{10}(80)$ and it converts PSD of CRd signal from 8 MHz to 100 kHz. Therefore, PU SNR values considered comprises of SNR_{TV} signal to Noise Ratio for the TV signal and the SNR_{PMSE} signal to Noise Ratio for the PMSE signal. The Table 1 shows the PMSE bandwidth and the associated power.

- Bandwidth of the channel: The TV broadcast system in a specific geographical location operates at a particular bandwidth. In the United Kingdom, TV broadcast channel has 8 MHz as bandwidth and this information is employed for training the ASA-NN as a second input. In addition to that, the bandwidth of the probable PMSE devices operating in the TV white space is also considered.
- Centre Frequency of the channels: The employed centre frequency for training NN is as TV white space frequencies as shown in Figure 9.
- Cyclic Frequency (cyclostationary features of the signal): The periodicity in a signal or in its mean and autocorrelation results in the cyclostationary properties. The noise signal can be differentiated from the PU signal by employing the cyclo-

stationary property. The wide sense stationary noise signals exhibit no correlation where as modulated PU signal exhibits correlation due to periodic nature of the signals [13]. The cyclic spectral density of the received PU signal during spectrum sensing in Equation (1) can be calculated as in Equation (40) [57]:

$$S(f, \alpha) = \sum_{r=-\infty}^{\infty} R_y^\alpha(\tau) e^{-j2\pi f\tau}, \quad (40)$$

where $R_y^\alpha(\tau)$ can be calculated as in Equation (41):

$$R_y^{\alpha_a}(\tau) = E[y(n+\tau)y^*(n-\tau)]e^{j2\pi\alpha_a n}, \quad (41)$$

here α_a is the cyclic frequency. When cyclic frequency is equal to fundamental frequency of the signal then cyclic spectral density shows peak [5]. In addition to that, noise signals which are wide sense stationary does not have any periodicity associated with it, so their autocorrelation function is [58].

$$R_y(\tau) = R_y^0(\tau). \quad (42)$$

As the cyclostationary signals comprises periodicity, therefore, their autocorrelation function can be written as

$$R_y(\tau) = \sum_{r=-\infty}^{\infty} R_y^\alpha(\tau) e^{j2\pi\alpha_a \tau}, \quad (43)$$

where α_a is equivalent with period T :

$$\alpha_a = \frac{a}{T}, \quad a = 0, \pm 1, \pm 2, \dots \quad (44)$$

The cyclic frequency is used as one of the input feature for detecting the PU signal.

9 | SIMULATION PARAMETERS AND RESULTS

The simulation results depict the performance of ASA in training the NN for efficient spectrum sensing in terms of the probability of detection, probability of false alarm, opportunistic throughput, and the bit error rate (BER). The BER for different training algorithm is estimated based on the efficiency of each algorithm in predicting the accurate spectrum holes and transmitting the data efficiently to CR receiver.

The simulation parameters of each metaheuristic algorithm employed for training NN are as follows:

The number of CRs deployed in the vicinity of the airport is considered as 10, 5 aircraft is considered to be approaching ATC at a time, the number of spectrum sensing samples = 500. The TV tower transmission power is assumed to be vary from 10 to 50 kW depending on the geographical location of the place. The noise power spectral density is 10^{-9} , the PU bandwidth is 8 MHz. The CRs and CR base station are assumed to be within

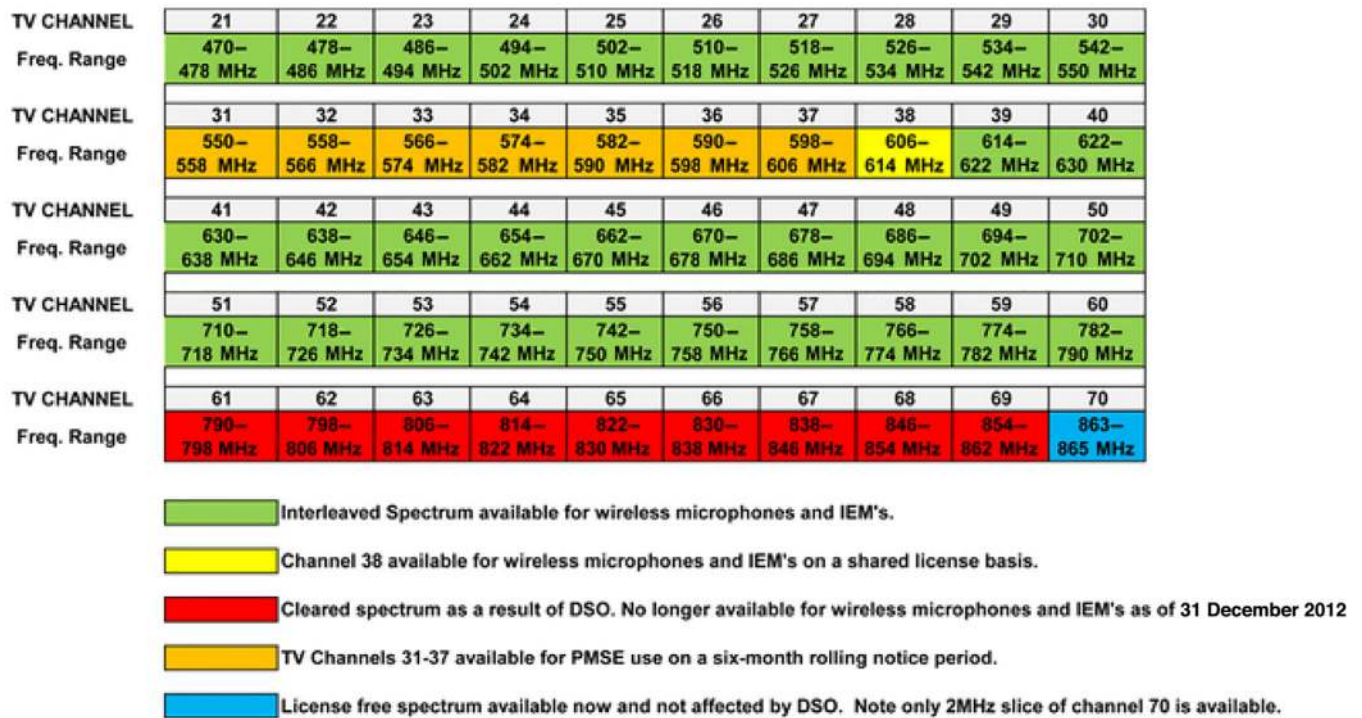


FIGURE 9 TV carrier frequency allocation in the United Kingdom [56]

TABLE 2 Simulation parameters of metaheuristic algorithms employed for training NN

PSO/PSOGSA	GSA	ABC	ASA
1. Personal Coefficient and Social Coefficient = $C_1 = C_2 = 2$	1. Gravitational Constant = 1	1. Population Size = 100	1. Population Size = 100
2. Inertia weight w = Linearly decreases from 0.9 to 0.4	2. Initial search agent velocity = [0,1]	2. Maximum Iteration = 500	2. Maximum Iteration = 500
3. Population Size = 100	3. Descending Coefficient = 20	3. Total NN Layer = 3	3. Gliding Constant = 1.9
4. Maximum Iteration = 500, Descending Coefficient = 20	4. Initial value of acceleration, mass of the search agents set to 0	4. Hidden Layer Size = 10	4. Random Gliding Distance = 9–20 m
5. $R_1, R_2 = [0,1]$	5. Population Size = 100		5. Scaling Factor = 16–37
6. Total NN Layers = 3	6. Maximum Iteration = 500		6. $\vartheta(0) = 1$
7. Hidden Layer Size = 10	7. Total NN Layers = 3		7. Total NN Layers = 3
8. Gravitational Constant = 1	8. Hidden Layer Size = 10		8. Hidden Layer Size = 10

the distance of 1 km from the TV transmission tower. The TV tower transmission range is assumed to be 2.5 km, the probability of PU being active is considered to be 0.1. The Table 2 shows the simulation parameters of metaheuristic algorithms employed for training the NN.

9.1 | Real-time training of NN with the help of USRP, LabVIEW, and MATLAB

The NN is first trained for the known samples of the received PU and PMSE SNR, the PU and PMSE centre frequency, PU cyclic frequency, PU and PMSE signal bandwidth. For the real-

time training, USRP N210 (Number of N210 = 2, USRP 1 and USRP 2) and B210 (Number of B210 = 1, USRP 3) are employed. In the training phase, USRP 1 and USRP 3 transmit at different SNR levels, bandwidth and carrier frequency so as to replicate the TV and PMSE transmission. The USRP 2 has the priori knowledge about the presence and the absence of PU signal, trains the NN using the sensed samples and trains the ASA-NN in the MATLAB environment.

During working phase, the USRP 2 act as the FC. The USRP 2 receives the sensed samples from USRP 1 and USRP 3, and is fed to ASA-trained NN in the MATLAB environment and makes the final decision. Figures 10 and 11 shows the test bench setup employed in this work. The training of NN starts with



FIGURE 10 USRP 1 and USRP 2 (N210s) placed at a distance of 4 m (Testbench for the proposed algorithm)

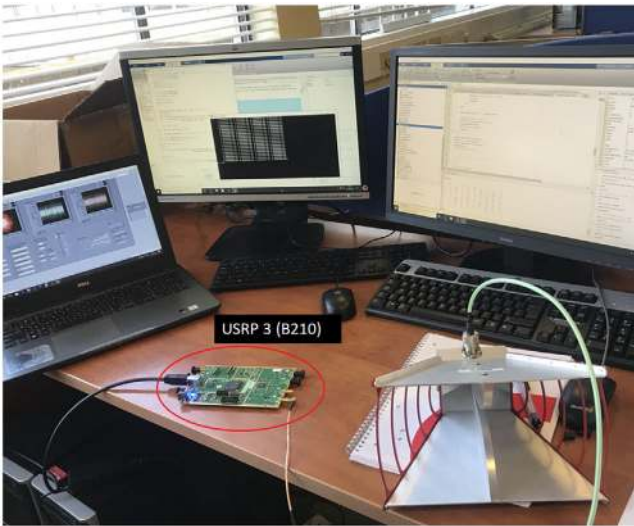


FIGURE 11 USRP 3 (B210) with horn antenna

random initialization of the weight and the bias values. During epoch 1, for the corresponding values of the weight and bias, the output is generated and compared with the target value (prior information about PU). The error value and the associated weight and the bias values are then called via applied optimization algorithms. After first iteration, the optimized weight and bias values for the minimized error value is fed back to the NN, which then generates the output and compared with the target. The error signal along with the weight and bias values are then again called by the optimization algorithm. The process continues until the target error minimization value has been reached or the iteration reaches the maximum level.

9.2 | Evaluation of the detection performance of the proposed and the existing algorithm

The detection performance of the proposed ASA-trained NN-based spectrum sensing is compared with the PSO-GSA-NN, PSO-NN, ABC-NN, GSA-NN, and Conventional-NN. The efficiency of the optimization algorithm in training NN is deduced by its effectiveness in optimizing the weight and bias

values of NN to minimize the error in correct detection of the spectrum holes. An efficient algorithm can successfully detect the presence and the absence of PU. The detection performance of the NN training algorithm is evaluated in terms of probability of detection. The better probability of detection signifies the efficiency of the algorithm in training the NN for the correct prediction about the presence and the absence of PU.

The probability of detection of each algorithm is evaluated with respect to probability of false alarm, sensing time, and the received SNR of the PU.

1. Impact of Probability of False Alarm on Probability of Detection for each Algorithm:

Figure 12 shows the receiver operating characteristics (ROC) for spectrum sensing with respect to probability of detection and probability of false alarm.

Once the NN is trained using proposed algorithm, then the probability of detection and probability of false alarm is plotted by employing the real-time spectrum sensing samples using USRP 2. The USRP 2 performs wide band spectrum sensing in the TV white space band (470–790 MHz). From the sensed samples, the received PU SNR, its bandwidth, cyclic frequency, and centre frequency is obtained. These samples are fed to the trained NN which predicts the presence and the absence of PU. For the particular SNR value and based on the NN prediction, the probability of detection is estimated via employing Equation (14). With the given SNR (SNR_{TV} and SNR_{PMSE}) and for the predicted probability of detection, the optimal detection threshold is estimated using Equation (45)

$$\lambda = Q_{d,j}^{P_{d,j}^{cs}(k)} \sigma^1 + \mu^1. \quad (45)$$

Employing the above equations (14 and 45), the probability of false alarm is estimated using Equation (13). From Figure 12, it can be seen that for the probability of false alarm = 0.1 and sensing time = 5 ms, the probability of detection for the ASA-trained NN is better as compared to the other algorithms. The probability of detection of ASA-NN is ~ 1 , whereas for PSO-GSA-NN it is ~ 0.9 . The

FIGURE 12 Probability of detection versus probability of false alarm for sensing time = 5 ms

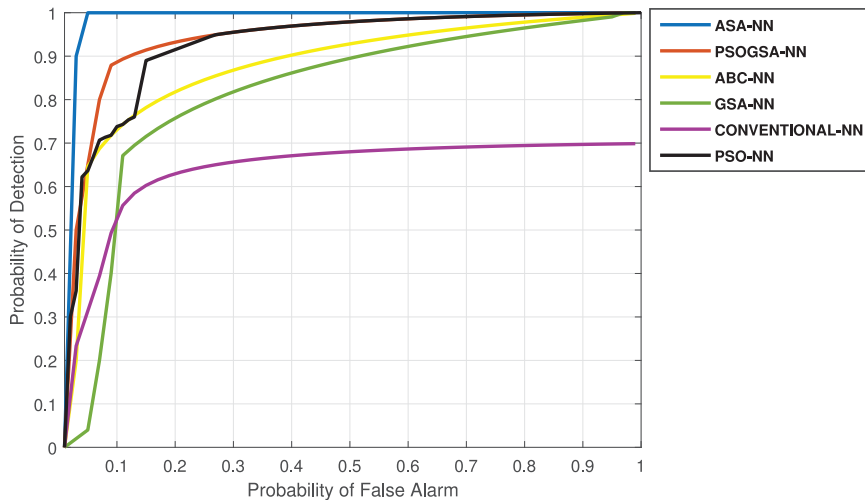
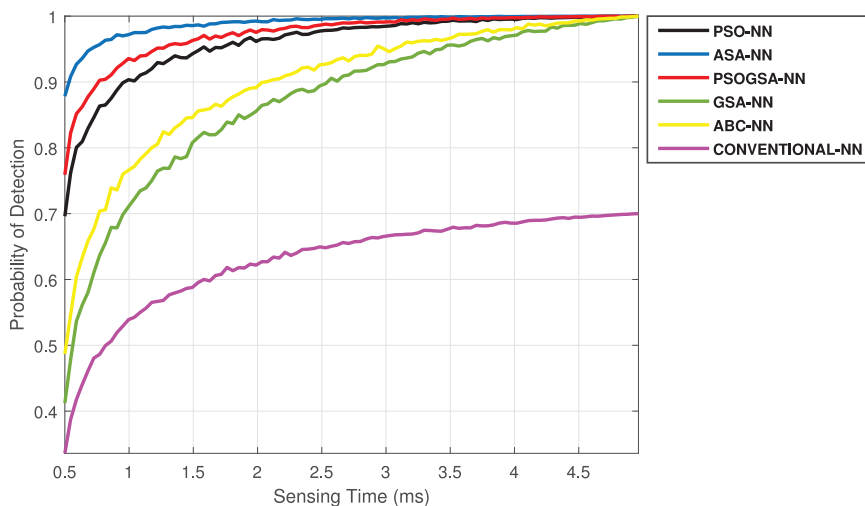


FIGURE 13 Probability of detection versus sensing time



PSO-NN has the comparable performance with the ABC-NN of about ~ 0.75 . The detection probability for the GSA-NN and Conventional-NN are ~ 0.6 and ~ 0.55 , respectively.

2. Impact of Probability of Sensing Time on Probability of Detection for each Algorithm: From Figure 13, it can be inferred that as the window of sensing time increases the probability of detection also increases. The increased sensing time increases the accuracy of the sensed data, eventually the prediction error reduces. But if the sensing time is kept increasing then the transmission time reduces which eventually reduces the opportunistic throughput and increases the energy consumption. Optimizing sensing time is another problem which we have dealt in our previous work. For a frame period of 50 ms the maximum sensing time considered is 5 ms. The detection performance of the proposed ASA-NN is better for varying sensing time as compared to the existing PSOGSA-NN, PSO-NN, ABC-NN, GSA-NN, and Conventional NN.
3. Impact of Probability of Received PU SNR on Probability of Detection for each Algorithm:

The PU SNR here comprises of SNR_{TV} and SNR_{PMSE} . Figure 14 shows the probability of detection for varying Received SNR values of PU signals. High SNR values guarantees better detection performance of the NN. The proposed ASA-NN is able to reach high detection probability of ~ 0.98 even at low SNR value of 0 dB. The proposed ASA-NN is very efficient in detecting the presence and absence of PU for both high as well as for low SNR, as compared to the existing algorithms.

4. Real-Time Detection of the Spectrum Holes using proposed ASA-NN.

Once NN is trained using ASA then the ASA-NN-based spectrum sensing is carried out using USRP 2, which act as FC. The FC receives sensed data from the USRP 1 and USRP 3. Based on the sensed samples and trained NN, the USRP 2 makes the final decision on the presence and the absence of the PU. Once the PU is detected then the threshold is varied based on Equations (13) and (14). The detected PU is then displayed via LabVIEW front panel GUI, as shown in Figures 15 and 16.

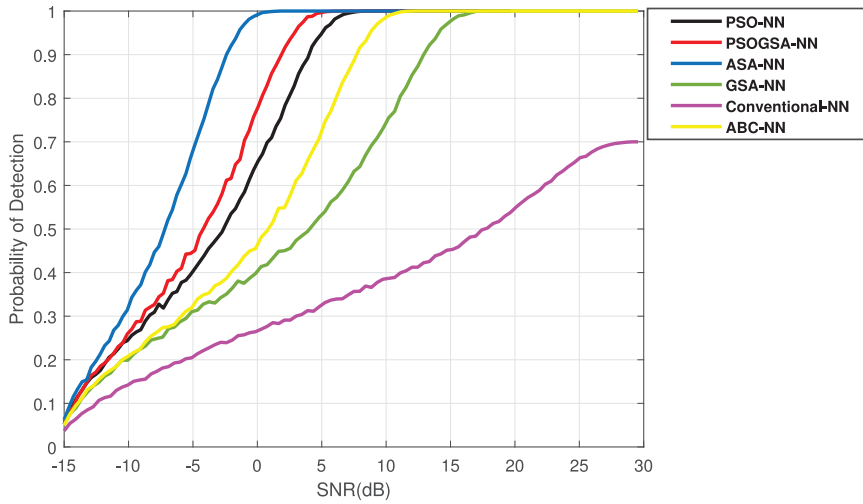


FIGURE 14 Probability of detection versus SNR (received SNR of PU)

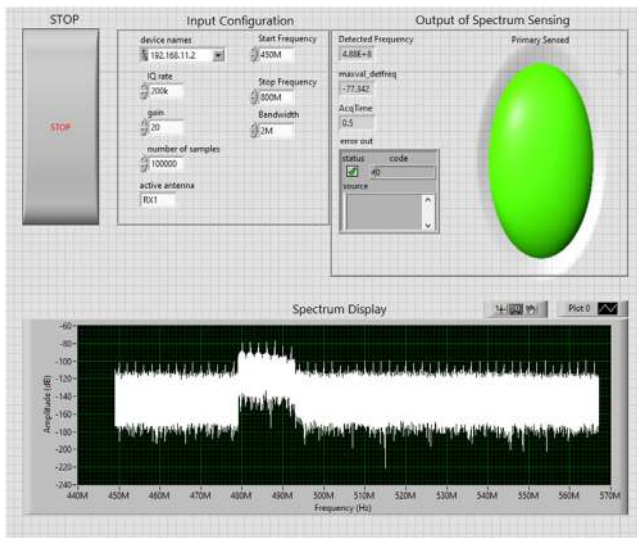


FIGURE 15 NI USRP-LabVIEW based detection of PU

9.3 | Evaluation of the transmission performance of the proposed and the existing algorithm

Based on how efficiently an algorithm-trained NN is able to detect the spectrum holes and effectively utilize it for the transmission of data, the performance is evaluated in terms of the BER and opportunistic throughput. The USRP 2 performs the spectrum sensing and detect the spectrum holes using optimization algorithm-trained NN and transmits the data to the USRP 3. The distance between USRP 2 and USRP 3 is varied so as to have different values for the received SU SNR.

1. ASA-NN based transmission of signals from USRP 2 to USRP 3 using different modulation scheme:
From Figures 17–19, it can be inferred that with the proposed ASA-NN it is possible to efficiently detect the spec-

trum holes and transmit data. The ASA has efficiently trained NN and has optimized the error in detection of the spectrum holes via its novel mutation, crossover, and chaotic winter selection scheme. The figures corresponding to the receiver USRP is accompanied by channel noise, but when there is interference with the noise the received signal is as shown in Figure 17 and it is very difficult to trace the original transmitted signal.

2. BER analysis of different optimization algorithm employed in training NN:

The efficiency of the optimization algorithm in training NN to effectively detect the spectrum holes is analysed with respect to BER as shown in Figures 20–22. From the BER analysis, it can be inferred that the proposed ASA-NN because of its crossover and mutation scheme is able to obtain optimum weight values for correctly detecting the spectrum holes and has efficiently transmitted data from USRP 2 to USRP 3.

3. Opportunistic throughput analysis of different optimization algorithm employed in training NN:

The opportunistic throughput of a CRN is the throughput obtained at SU receiver. This throughput is calculated as per Equation (15) for transmission of data via detected spectrum holes. Better detection of the spectrum holes results in enhanced throughput. Therefore, efficiency of the optimization algorithm in training NN for efficient prediction of the spectrum holes is analysed with respect to opportunistic throughput as shown in Figures 23–25.

9.4 | Comparative analysis of each algorithm

The comparative analysis of ASA-NN with the PSOGSA-NN, PSO-NN, ABC-NN, GSA-NN, and Conventional-NN is as shown in Tables 3–6. Table 3 shows performance evaluation of each NN training algorithm for probability of detection at probability of false alarm = 0.1. As discussed in the point 1 of Subsection 9.2, the ASA has effectively improved NN

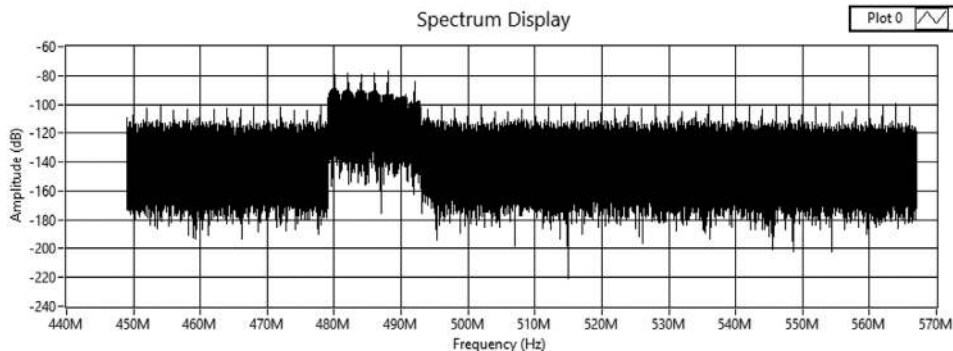


FIGURE 16 Detected PU in the TV band

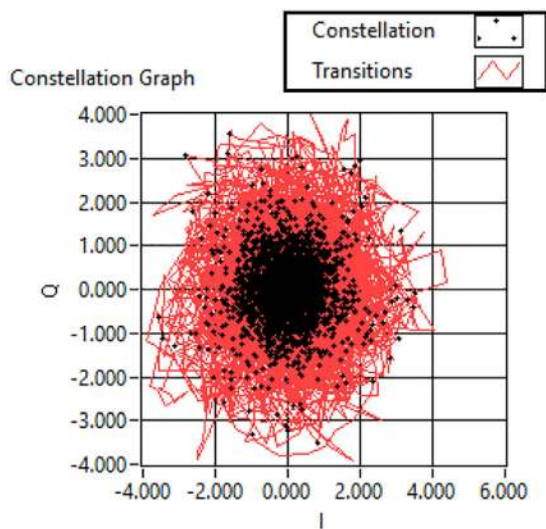


FIGURE 17 Signal (PU interference)

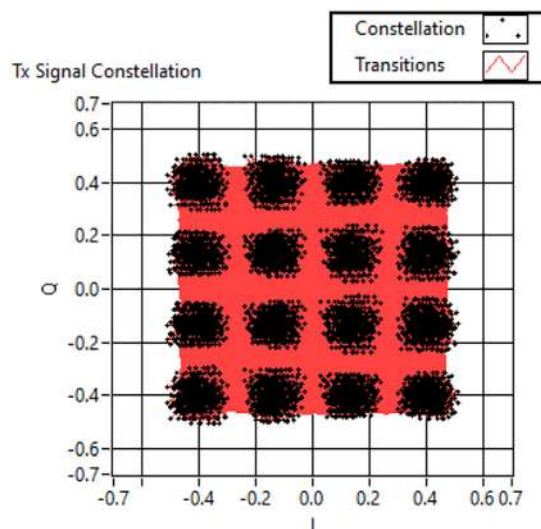


FIGURE 18 Transmission at 16 QAM

as compared to other optimization algorithm for efficiently detecting the presence and absence of PU. The ASA algorithm has the tremendous trade-off between its exploration and exploitation abilities. The chaotic behaviour introduced in ASA (Equation 26) has further enhanced its exploration ability with which it tends to find global optimum solution.

Table 4 depicts the performance evaluation of each training algorithm with respect to probability of detection and sensing time.

Table 5 shows the opportunistic throughput for each training algorithm for varying SNR at SU Rx. As the result of efficient spectrum prediction and data transmission, the opportunistic throughput of ASA-NN is better as compared to the PSO-GSA-NN, PSO-NN, ABC-NN, GSA-NN, and Conventional-NN.

In Tables 3, 4, 5, and 6, the performance of the proposed ASA-NN is compared with the existing (PSO-GSA-NN, PSO-NN, GSA-NN, and Conventional-NN) for parameters (Varying P_f , sensing time, and SNR). Table 7 shows by how much percentage there is improvement in the Probability of Detection and opportunistic throughput using ASA-NN as compared to the existing (PSO-GSA-NN, PSO-NN, GSA-NN, and Conventional-NN). From the best of authors' knowledge, so far

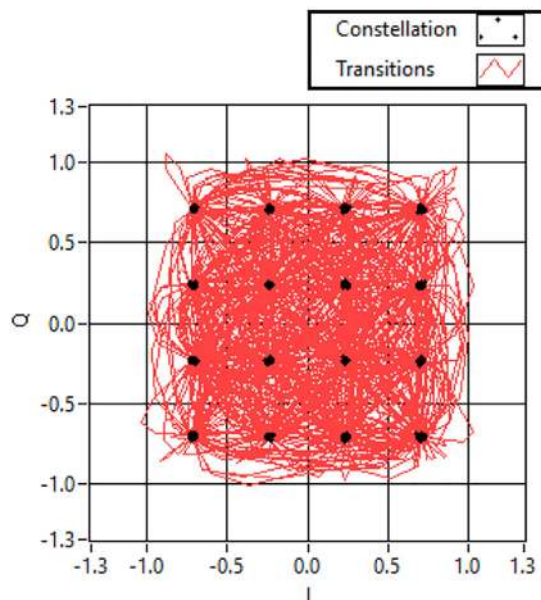


FIGURE 19 Reception at 16 QAM

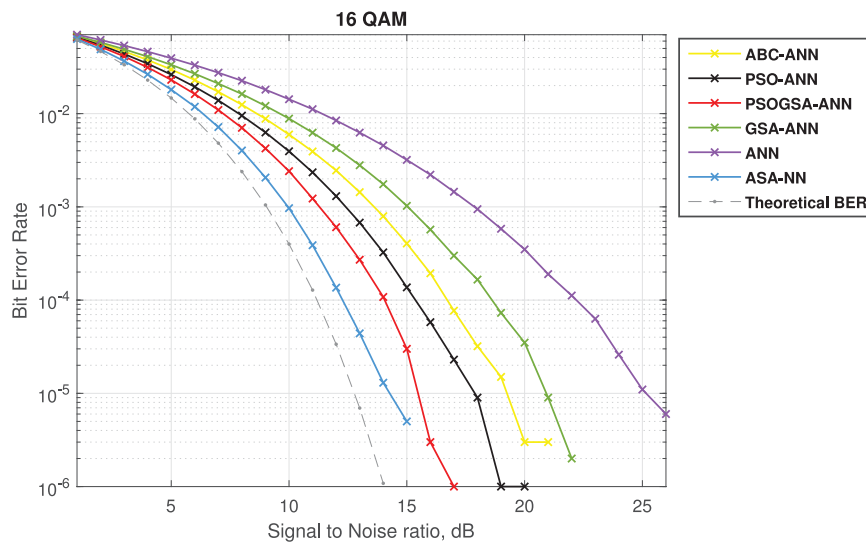


FIGURE 20 BER for 16 QAM

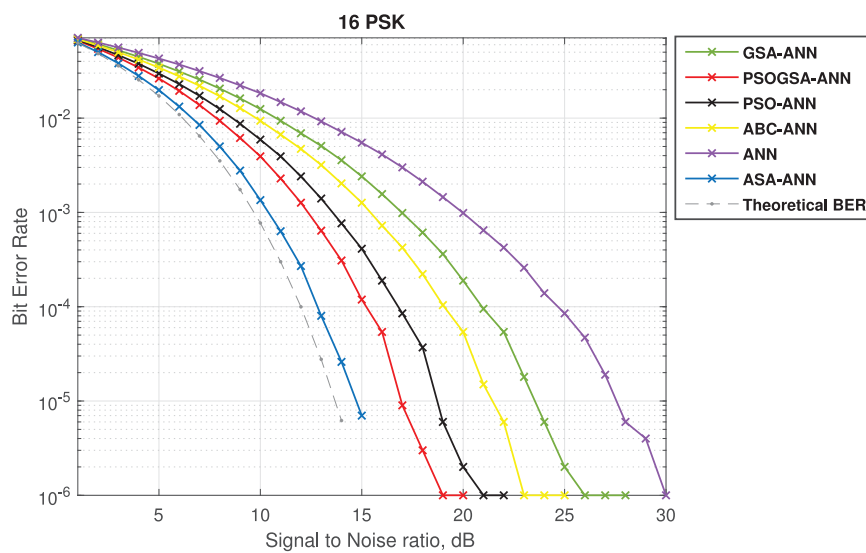


FIGURE 21 BER for 16 PSK

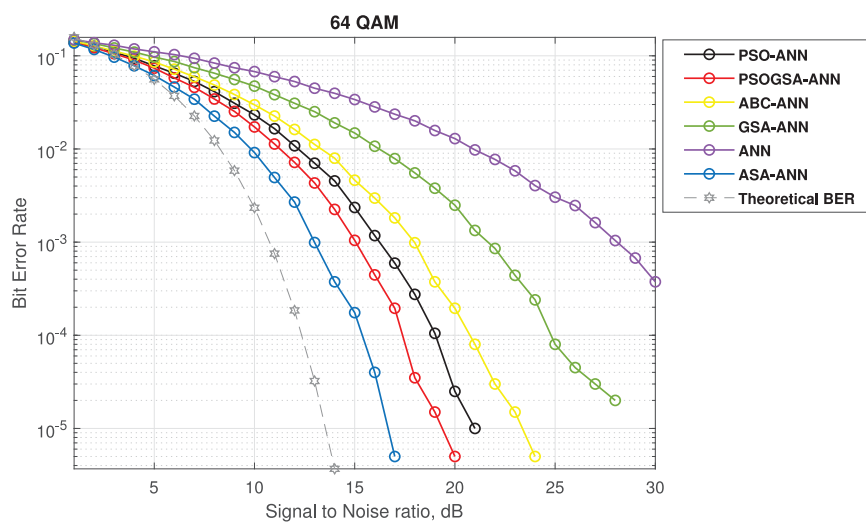


FIGURE 22 BER for 64 QAM

FIGURE 23 Opportunistic throughput versus SNR for 16 QAM

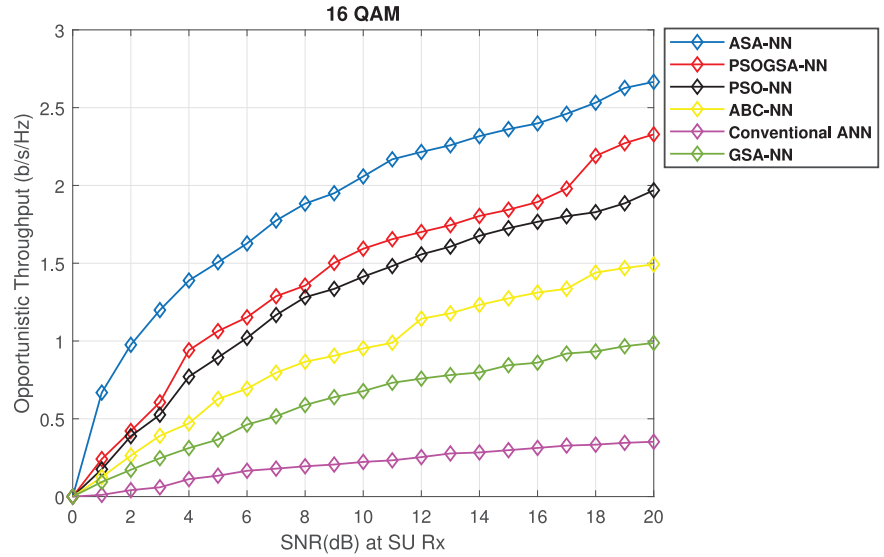


FIGURE 24 Opportunistic throughput versus SNR for 16 PSK

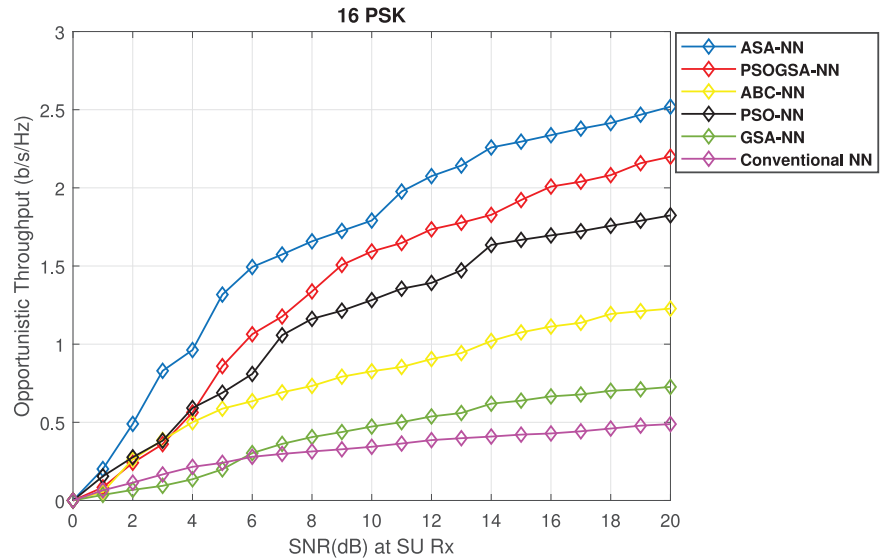


FIGURE 25 Opportunistic throughput versus SNR for 64 QAM

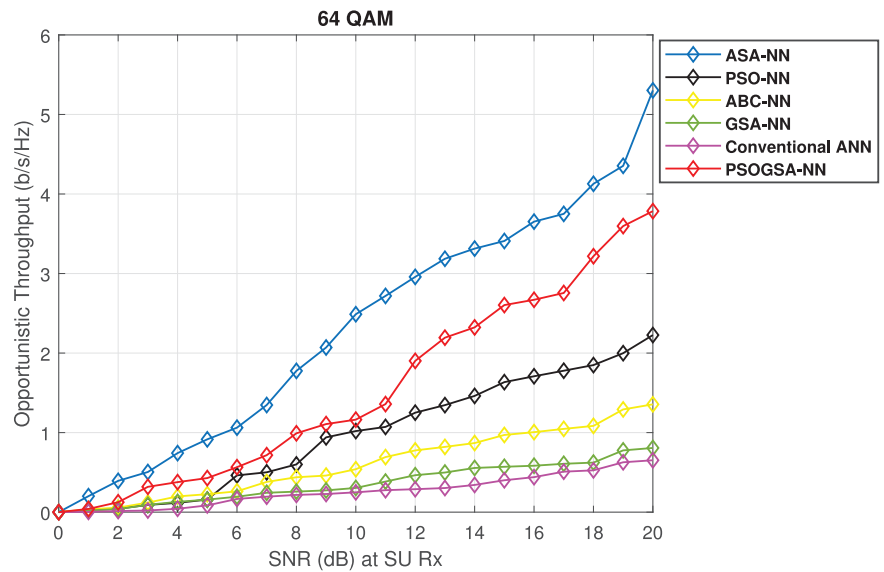


TABLE 3 Performance evaluation with respect to probability of detection and probability of false alarm

Probability of detection at $P_f = 0.1$					
ASA-NN	PSOGSA-NN	PSO-NN	ABC-NN	GSA-NN	Conventional-NN
~ 1	~ 0.9	0.75	0.738	0.6	0.54

TABLE 4 Performance evaluation with respect to probability of detection and sensing time

Probability of detection at sensing time = 1 ms					
ASA-NN	PSOGSA-NN	PSO-NN	ABC-NN	GSA-NN	Conventional-NN
~ 1	0.93	0.9	0.76	0.71	0.53

in the spectrum sensing based on NNs were carried for either P_d versus SNR [59], or P_d versus P_f [60, 61] or, P_d versus sensing time. All the three parameters are considered simultaneously (Tables 3–6) to prove the efficacy of the proposed algorithm.

9.5 | Convergence curve analysis

The convergence curve signifies the convergence of the optimization algorithm towards the best values of the variables

TABLE 5 Performance evaluation with respect to probability of detection and SNR

Probability of detection at received PU SNR = 0 dB					
ASA-NN	PSOGSA-NN	PSO-NN	ABC-NN	GSA-NN	Conventional-NN
0.98	0.8067	0.6556	0.48	0.39	0.26

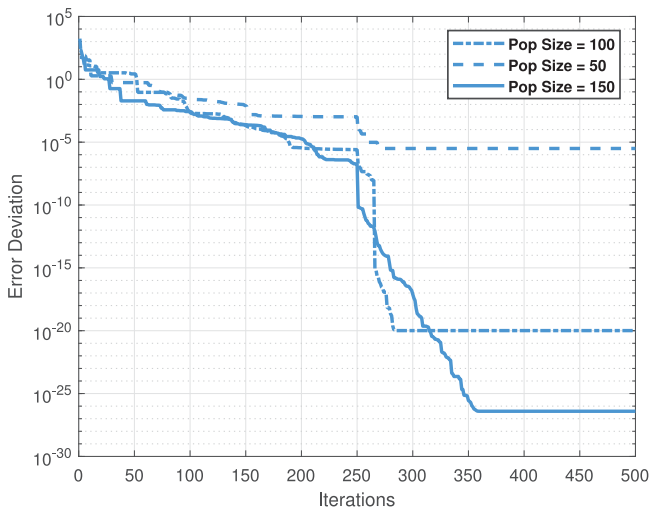


FIGURE 26 Convergence curve of ASA-NN for population size 50, 100, 150

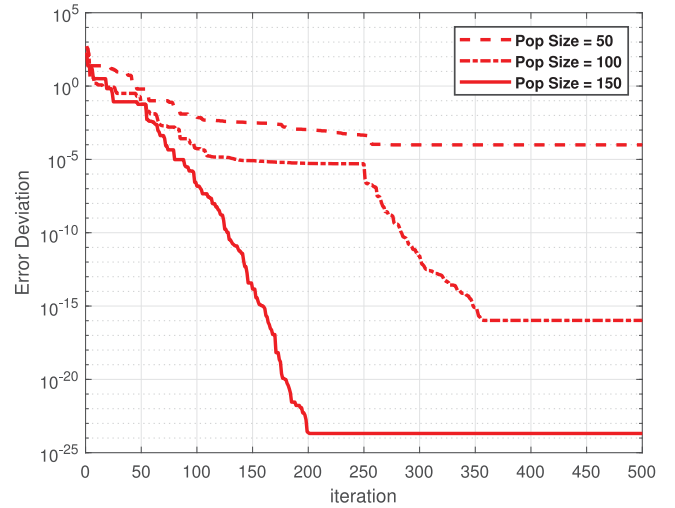


FIGURE 27 Convergence curve of PSOGSA-NN for population size 50, 100, 150

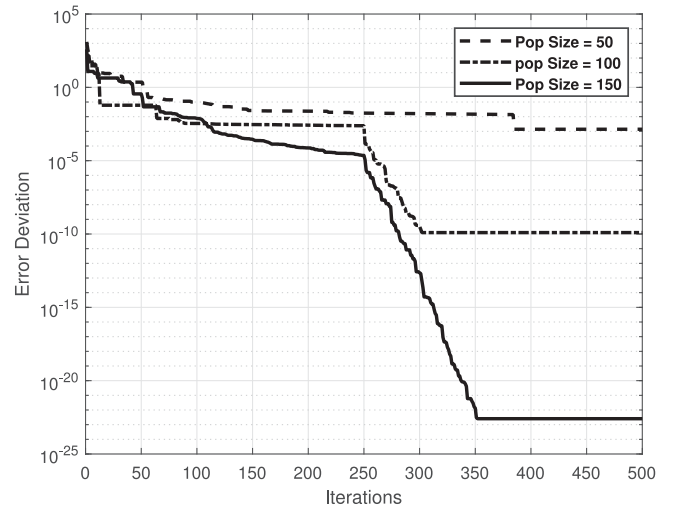


FIGURE 28 Convergence curve of PSO-NN for population size 50, 100, 150

resulting in the minimization/maximization of the objective function. The aim of each optimization algorithm is to train the NN by optimizing the weights of NN so as to obtain the minimized error deviation between the observed and the target sample values. The training is carried out in the training period, the trained NN is then implied for predicting the PU’s presence and absence.

The convergence curve is an important paradigm showing the efficiency of the optimization algorithm during the training phase of an NN. The optimization algorithm having minimized error deviation at the end of the training phase iterations implies that the algorithm has obtained optimum weight values for which the deviation between the observed and the target value is minimum and has trained the NN in best way. The optimal trained NN can efficiently detect the presence and the absence of PU during the working phase.

TABLE 6 Opportunistic throughput for varying SNR at SU Rx

S.No.	Modulation scheme	Opportunistic throughput (b/s/Hz)					
		ASA-NN	PSOGSA-NN	PSO-NN	ABC-NN	GSA-NN	Conventional-NN
1	16 QAM	2.66	2.32	1.96	1.49	1	0.35
2	16 PSK	2.51	2.199	1.82	1.22	0.72	0.48
3	64 QAM	5.3	3.78	2.226	1.355	0.807	0.652

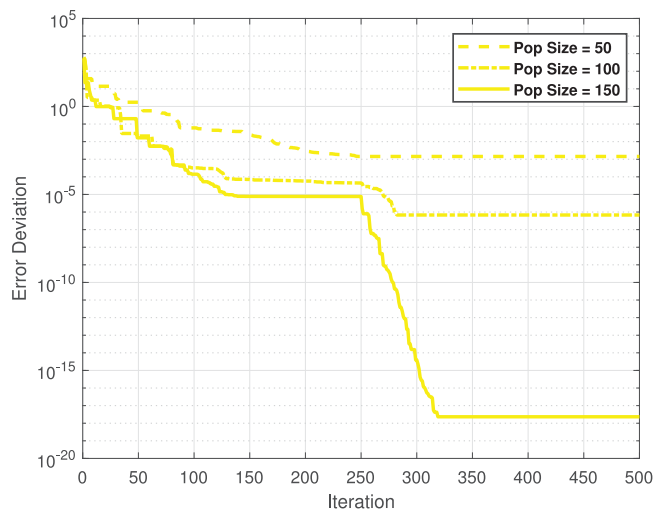
TABLE 7 Percentage improvement of the proposed ASA-NN as compared to the existing algorithms for different parameters

Existing Algorithms	Probability of detection at $P_f = 0.1$	Probability of detection at sensing time = 1 ms	Probability of detection at received PU SNR = 0 dB	Opportunistic throughput at 16 QAM
PSOGSA-NN	11.11%	7.52%	21.48%	14.60%
PSO-NN	33.33%	11%	50.76%	35.02%
ABC-NN	35.50%	31.50%	104.10%	78.50%
GSA-NN	67%	40.80%	151.20%	166%
Conventional-NN	85.18%	88.60%	276.90%	650%

Figure 26 shows the convergence curve of the ASA-NN for the population size 50, 100, 150. It can be seen that as the population size of an optimization algorithm increases, it converges towards better solution, i.e. minimum error deviation. But increasing population size to a very large value can increase the computational time during the training phase.

Similarly Figures 27–31 shows the convergence curve for the PSOGSA-NN, PSO-NN, ABC-NN, GSA-NN, and Conventional-NN, respectively. From these figures, it can be inferred that the population size enhances performance of an optimization algorithm.

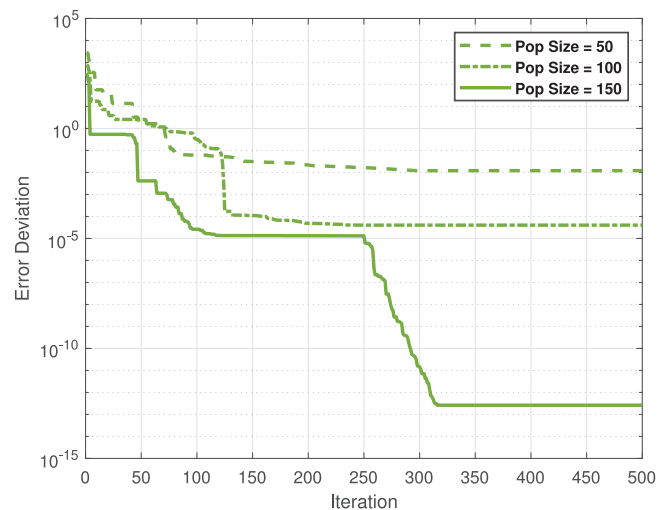
The combined comparative analysis of the convergence curve of each algorithm for the population size = 150 is shown in Figure 32. Each algorithm is then analytically viewed via Table 8.

**FIGURE 29** Convergence curve of ABC-NN for population size 50, 100, 150

From Figure 32 and Table 8 it can be seen that the ASA-NN has shown significant improvement as compared to the existing PSOGSA-NN, PSO-NN, ABC-NN, GSA-NN and Conventional-NN. ASA-NN has shown 96.8% improvement as compared to PSOGSA-NN for the population size 50.

10 | DISCUSSION

In this work, NN is used for spectrum prediction, and from the best of our knowledge ASA has been employed for the first time for training the NN. The question arises on the use of the NN for spectrum prediction. In Section 2, the drawbacks associated with the conventional spectrum sensing have been discussed, which pointed towards enhancing the performance

**FIGURE 30** Convergence curve of GSA-NN for population size 50, 100, 150

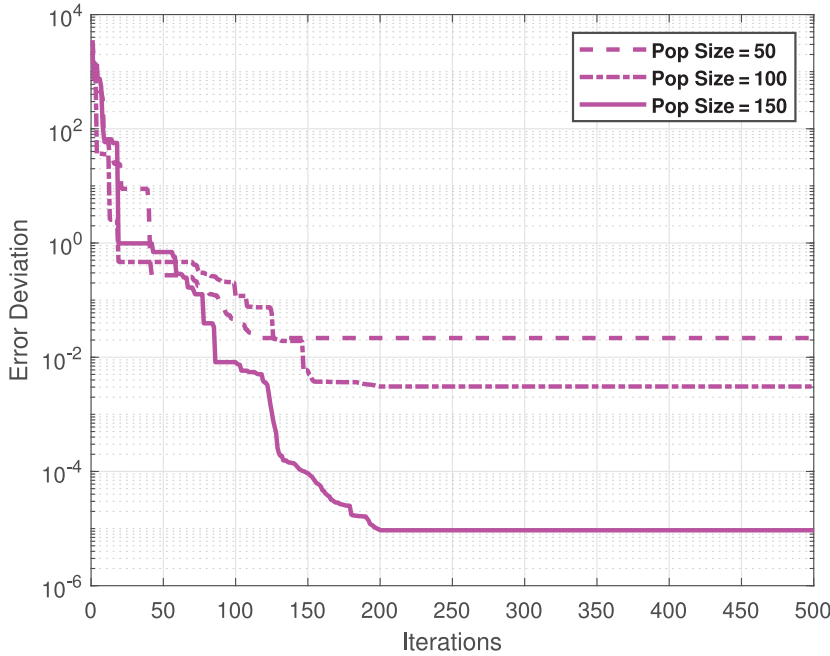


FIGURE 31 Convergence curve of the Conventional-NN for population size 50, 100, 150

TABLE 8 Converged error deviation for different population size of each training algorithm

S.No.	Training algorithm	Population size	Error deviation
1	ASA-NN	50	3.13×10^{-6}
		100	1.02×10^{-20}
		150	3.92×10^{-27}
2	PSOGSA-NN	50	9.78×10^{-5}
		100	1.04×10^{-16}
		150	2.05×10^{-24}
3	PSO-NN	50	1.30×10^{-3}
		100	1.24×10^{-10}
		150	2.55×10^{-23}
4	ABC-NN	50	1.40×10^{-3}
		100	6.78×10^{-7}
		150	2.32×10^{-18}
5	GSA-NN	50	1.20×10^{-2}
		100	4.02×10^{-5}
		150	2.62×10^{-13}
6	Conventional-NN	50	2.10×10^{-2}
		100	3.07×10^{-3}
		150	9.34×10^{-6}

of the conventional spectrum sensing. Therefore, the NN is employed to enhance the performance of conventional energy detector. The conventional energy detector has very poor performance in low SNR. The other spectrum sensing techniques like the MF and cyclostationary detector are highly complex, so it is not preferred to employ NN on those techniques [17]. The NN once trained using ASA in the training period, can efficiently be employed for spectrum prediction during the

working period. This can reduce processing delays and improve the efficiency of spectrum utilization.

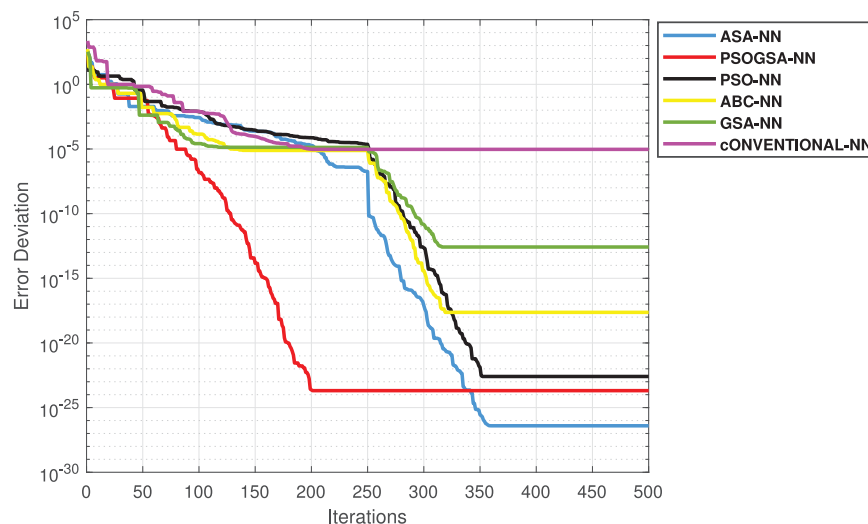
Another important question arises, why NN-based spectrum prediction should be preferred over conventional spectrum sensing with optimized parameters? The different optimization algorithms have been employed for improving the conventional spectrum sensing techniques [40, 62, 63]. In addition to that, the joint optimization scheme has also been employed for improving the energy detection-based spectrum sensing [64, 65]. These optimization schemes can only optimize the parameters of spectrum sensing technique but cannot completely mitigate the drawbacks associated with it, and NN has better convergence towards the desired solution as compared to optimization algorithms [66].

The Conventional-NN using gradient descent-based BP scheme has the tendency of sticking to the local optima solution [22–24]. Therefore, the ASA-NN, because of its excellent exploitation and exploration abilities has been employed for the efficient spectrum prediction. The spectrum prediction performed by ASA-NN has outperformed the PSOGSA-NN, PSO-NN, ABC-NN, GSA-NN and Conventional-NN in terms of improved ROC (Figure 12), high detection probability with respect to sensing time (Figure 13), improved detection probability with respect to SNR (Figure 14), better BER (Figures 20–22), and better opportunistic throughput (Figures 23–25).

11 | CONCLUSION

The issue of spectrum congestion during air traffic control has been investigated, and 3D NCSS and cooperative spectrum sensing have been proposed in this article. To overcome the drawbacks associated with conventional spectrum sensing, the novel Advanced Squirrel Search Algorithm-trained NN has

FIGURE 32 Combined convergence curve of different algorithm for population size 150



been proposed for efficient spectrum prediction in CRN-based air traffic control. The efficiency of ASA-NN during training phase is evaluated in terms the ROC and probability of detection with respect to sensing time and SNR(PU+PMSE). The proposed ASA-NN has shown high detection probability and spectrum hole prediction as compared to the PSOGSA-NN, PSO-NN, ABC-NN, GSA-NN, and Conventional-NN. The efficacy of the proposed scheme for the real-time scenario is checked via implementing ASA-NN-based spectrum sensing via USRP N210 B210, LabVIEW 2018, and MATLAB 2019. The proposed ASA-NN has effectively detected the presence and the absence of the PU in real-time scenario. The proposed scheme has shown high opportunistic throughput and better BER (evaluated post-detection of the spectrum holes and transferring data) as compared to the PSOGSA-NN, PSO-NN, ABC-NN, GSA-NN, and Conventional-NN. The proposed spectrum sensing scheme with ASA-NN can be employed for efficiently detecting the spectrum holes for Air Traffic Control and thus overcoming the problem of spectrum congestion.

COMPLIANCE WITH ETHICAL STANDARDS

- 1 Conflict of Interest: First author, Mr. Geoffrey Eappen declares that he has no conflict of interest. Second author, Dr. Shankar T declares that he has no conflict of interest.
- 2 Ethical Approval: This article does not contain any studies with animals performed by any of the authors.

ORCID

Rajagopal Nilavalan  <https://orcid.org/0000-0001-8168-2039>

REFERENCES

1. Jacob, P., et al.: Cognitive radio for aeronautical communications: A survey. *IEEE Access* 4, 3417–3443 (2016)
2. Chiang, R.I.C., Rowe, G.B., Sowerby, K.W.: A quantitative analysis of spectral occupancy measurements for cognitive radio. In: *IEEE 65th Vehicular Technology Conference - VTC2007-Spring*, pp. 3016–3020. IEEE (2007)
3. Wellens, M., Wu, J., Mahonen, P.: Evaluation of spectrum occupancy in indoor and outdoor scenario in the context of cognitive radio. In: *2nd International Conference on Cognitive Radio Oriented Wireless Networks and Communications*, pp. 420–427. IEEE (2007)
4. Erpek, T., Steadman, K., Jones, D.: Dublin Ireland Spectrum Occupancy Measurements Collected on April 16-18, 2007. The Shared Spectrum Company (2007)
5. Yucek, T., Arslan, H.: Spectrum characterization for opportunistic cognitive radio systems. In: *MILCOM 2006-2006 IEEE Military Communications Conference*, pp. 1–6. IEEE (2006)
6. Shreejith, S., et al.: Efficient spectrum sensing for aeronautical LDACS using low-power correlators. *IEEE Trans. Very Large Scale Integr. VLSI Syst.* 26 (6), 1183–1191 (2018)
7. Kamali, B.: An overview of VHF civil radio network and the resolution of spectrum depletion. In: *Integrated Communications, Navigation, and Surveillance Conference Proceedings*, pp. 4–5. IEEE (2010)
8. Marcus, M., et al.: Federal communications commission spectrum policy task force. Report of the Unlicensed Devices and Experimental Licenses Working Group (2002)
9. Lee, W.-Y., Akyildiz, I.F.: Optimal spectrum sensing framework for cognitive radio networks. *IEEE Trans. Wireless Commun.* 7 (10), 3845–3857 (2008)
10. Proakis, J.G., Salehi, M.: *Digital Communications*, vol. 4. McGrawhill, New York (2001)
11. Zeng, Y., Liang, Y.-C.: Eigenvalue-based spectrum sensing algorithms for cognitive radio. *IEEE Trans. Commun.* 57 (6), 1784–1793 (2009)
12. Urkowitz, H.: Energy detection of unknown deterministic signals. *Proc. IEEE* 55 (4), 523–531 (1967)
13. Cabric, D., Mishra, S.M., Brodersen, R.W.: Implementation issues in spectrum sensing for cognitive radios. In: *Conference Record of the Thirty-Eighth Asilomar Conference on Signals, Systems and Computers*, vol. 1, pp. 772–776. IEEE (2004)
14. Subhedar, M., Birajdar, G.: Spectrum sensing techniques in cognitive radio networks: A survey. *Int. J. Next-Gener. Networks* 3 (2), 37–51 (2011)
15. Lin, Z., et al.: A energy prediction based spectrum sensing approach for cognitive radio networks. In: *5th International Conference on Wireless Communications, Networking and Mobile Computing*, pp. 1–4. IEEE (2009)
16. Tumuluru, V.K., Wang, P., Niyato, D.: A neural network based spectrum prediction scheme for cognitive radio. In: *IEEE International Conference on Communications*, pp. 1–5. IEEE (2010)

17. Tumuluru, V.K., Wang, P., Niyato, D.: Channel status prediction for cognitive radio networks. *Wireless Commun. Mobile Comput.* 12 (10), 862–874 (2012)
18. Xing, X., et al.: Channel quality prediction based on Bayesian inference in cognitive radio networks. In: *Proceedings IEEE INFOCOM*, pp. 1465–1473. IEEE (2013)
19. Xing, X., et al.: Spectrum prediction in cognitive radio networks. *IEEE Wireless Commun.* 20 (2), 90–96 (2013)
20. Clancy, C., et al.: Applications of machine learning to cognitive radio networks. *IEEE Wireless Commun.* 14 (4), 47–52 (2007)
21. Zhang, T., Wu, M., Liu, C.: Cooperative spectrum sensing based on artificial neural network for cognitive radio systems. In: *8th International Conference on Wireless Communications, Networking and Mobile Computing*, pp. 1–5. IEEE (2012)
22. Kartalopoulos, S.V., Kartakopoulos, S.V.: *Understanding Neural Networks and Fuzzy Logic: Basic Concepts and Applications*. Wiley-IEEE Press (1997)
23. Kayarvizhy, N., Kanmani, S., Uthariaraj, V.R.: ANN models optimized using swarm intelligence algorithms. *WSEAS Trans. Comput.* 45 (13), 501–519 (2014)
24. Narendra, K.S., Parthasarathy, K.: Identification and control of dynamical systems using neural networks. *IEEE Trans. Neural Networks* 1 (1), 4–27 (1990)
25. Da, Y., Xiurun, G.: An improved PSO-based ANN with simulated annealing technique. *Neurocomputing* 63, 527–533 (2005)
26. Karaboga, D., Akay, B., Ozturk, C.: Artificial bee colony (ABC) optimization algorithm for training feed-forward neural networks. In: *International Conference on Modeling Decisions for Artificial Intelligence*, pp. 318–329. Springer (2007)
27. Mirjalili, S., Hashim, S.Z.M., Sardroudi, H.M.: Training feedforward neural networks using hybrid particle swarm optimization and gravitational search algorithm. *Appl. Math. Comput.* 218 (22), 11125–11137 (2012)
28. Jadidi, Z., et al.: Flow-based anomaly detection using neural network optimized with GSA algorithm. In: *IEEE 33rd International Conference on Distributed Computing Systems Workshops*, pp. 76–81. IEEE (2013)
29. Yang, X.-S.: *Nature-Inspired Metaheuristic Algorithms*. Luniver Press (2010)
30. Yang, X.: Swarm intelligence based algorithms: A critical analysis. *Evol. Intell.* 7 (1), 17–28 (2014)
31. Yang, X.-S., et al.: *Metaheuristics in Water, Geotechnical and Transport Engineering*. Newnes (2012)
32. Ma, J., Zhao, G., Li, Y.: Soft combination and detection for cooperative spectrum sensing in cognitive radio networks. *IEEE Trans. Wireless Commun.* 7 (11), 4502–4507 (2008)
33. Quan, Z., Cui, S., Sayed, A.H.: Optimal linear cooperation for spectrum sensing in cognitive radio networks. *IEEE J. Sel. Top. Signal Process.* 2 (1), 28–40 (2008)
34. Shen, F., et al.: UAV-based 3D spectrum sensing in spectrum-heterogeneous networks. *IEEE Trans. Veh. Technol.* 68 (6), 5711–5722 (2019)
35. Duan, D., Yang, L., Principe, J.C.: Cooperative diversity of spectrum sensing for cognitive radio systems. *IEEE Trans. Signal Process.* 58 (6), 3218–3227 (2010)
36. Liu, X., et al.: Spectrum sensing optimization in an UAV-based cognitive radio. *IEEE Access* 6, 44002–44009 (2018)
37. Saleem, Y., Rehmani, M.H., Zeadally, S.: Integration of cognitive radio technology with unmanned aerial vehicles: Issues, opportunities, and future research challenges. *J. Network Comput. Appl.* 50, 15–31 (2015)
38. Liang, X., et al.: Throughput optimization for cognitive UAV networks: A three-dimensional-location-aware approach. *IEEE Wireless Commun. Lett.* 9(7), 948–952 (2020)
39. Wu Jun, et al.: Optimisation of virtual cooperative spectrum sensing for UAV-based interweave CR system. *IET Communications*(2020). <http://doi.org/10.1049/iet-com.2020.0252>
40. Eappen, G., Shankar, T.: Hybrid PSO-GSA for energy efficient spectrum sensing in cognitive radio network. *Phys. Commun.* 40, 101091 (2020)
41. Liang, Y.-C., et al.: Sensing-throughput tradeoff for cognitive radio networks. *IEEE Trans. Wireless Commun.* 7 (4), 1326–1337 (2008)
42. Jain, M., Singh, V., Rani, A.: A novel nature-inspired algorithm for optimization: Squirrel search algorithm. *Swarm Evol. Comput.* 44, 148–175 (2019)
43. Wolpert, D.H., Macready, W.G.: No free lunch theorems for optimization. *IEEE Trans. Evol. Comput.* 1 (1), 67–82 (1997)
44. Palyulin, V.V., Chechkin, A.V., Metzler, R.: Lévy flights do not always optimize random blind search for sparse targets. *Proc. Natl. Acad. Sci.* 111 (8), 2931–2936 (2014)
45. Eberhart, R., Kennedy, J.: A new optimizer using particle swarm theory. In: *MHS'95: Proceedings of the Sixth International Symposium on Micro Machine and Human Science*, pp. 39–43. IEEE (1995)
46. Rashedi, E., Nezamabadi-Pour, H., Saryazdi, S.: GSA: A gravitational search algorithm. *Inf. Sci.* 179 (13), 2232–2248 (2009)
47. Mirjalili, S., Hashim, S.Z.M.: A new hybrid PSOGSA algorithm for function optimization. In: *International Conference on Computer and Information Application*, pp. 374–377. IEEE (2010)
48. Karaboga, D., Akay, B.: A comparative study of artificial bee colony algorithm. *Appl. Math. Comput.* 214 (1), 108–132 (2009)
49. García-Ródenas, R., Linares, L.J., López-Gómez, J.A.: A memetic chaotic gravitational search algorithm for unconstrained global optimization problems. *Appl. Soft Comput.* 79, 14–29 (2019)
50. Zhang, X., Zou, D., Shen, X.: A novel simple particle swarm optimization algorithm for global optimization. *Mathematics* 6 (12), 287 (2018)
51. Bendov, O.: Transmitter SNR for maximum coverage. *IEEE Trans. Broadcast.* 54 (4), 784–785 (2008)
52. Goldsmith, A.: *Wireless Communications*. Cambridge University Press (2005)
53. Martin, S.R.: Tests of ATSC 8-VSB reception performance of consumer digital television receivers available in 2005. *FCC/OET TR 05-1017** (2005)
54. Sachs, J., Maric, I., Goldsmith, A.: Cognitive cellular systems within the TV spectrum. In: *IEEE Symposium on New Frontiers in Dynamic Spectrum (DySPAN)*, pp. 1–12. IEEE (2010)
55. Karimi, H.R.: A framework for calculation of TV white space availability subject to the protection of DTT and PMSE. In: *IEEE 24th Annual International Symposium on Personal, Indoor, and Mobile Radio Communications (PIMRC)*, pp. 2753–2758. IEEE (2013)
56. SHURE: Important information about wireless frequencies in U.K. <https://www.shure.com/en-GB/support/wireless-spectrum> (2020)
57. Maeda, K., et al.: Recognition among OFDM-based systems utilizing cyclostationarity-inducing transmission. In: *2nd IEEE International Symposium on New Frontiers in Dynamic Spectrum Access Networks*, pp. 516–523. IEEE (2007)
58. Napolitano, A.: *Generalizations of Cyclostationary Signal Processing*, vol. 95. Wiley (2012)
59. Tang, Y.-J., Zhang, Q.-Y., Lin, W.: Artificial neural network based spectrum sensing method for cognitive radio. In: *6th International Conference on Wireless Communications Networking and Mobile Computing (WiCOM)*, pp. 1–4. IEEE (2010)
60. Zheng, S., Lou, C., Yang, X.: Cooperative spectrum sensing using particle swarm optimisation. *Electron. Lett.* 46 (22), 1525–1526 (2010)
61. Li, X., et al.: Cooperative spectrum sensing based on an efficient adaptive artificial bee colony algorithm. *Soft Comput.* 19 (3), 597–607 (2015)
62. Azmat, F., Chen, Y., Stocks, N.: Bio-inspired collaborative spectrum sensing and allocation for cognitive radios. *IET Commun.* 9 (16), 1949–1959 (2015)
63. Rashid, R.A., et al.: Efficient in-band spectrum sensing using swarm intelligence for cognitive radio network. *Can. J. Electr. Comput. Eng.* 38 (2), 106–115 (2015)

64. Paysarvi-Hoseini, P., Beaulieu, N.C.: Optimal wideband spectrum sensing framework for cognitive radio systems. *IEEE Trans. Signal Process.* 59 (3), 1170–1182 (2010)
65. Luo, L., Roy, S.: Efficient spectrum sensing for cognitive radio networks via joint optimization of sensing threshold and duration. *IEEE Trans. Commun.* 60 (10), 2851–2860 (2012)
66. Jeffrey, W., Rosner, R.: Optimization algorithms – Simulated annealing and neural network processing. *Astrophys. J.* 310, 473–481 (1986)
67. Eappen Geoffrey, Shankar T A Survey on Soft Computing Techniques for Spectrum Sensing in a Cognitive Radio Network. *SN Computer Science* 1, (6), (2020) [.http://doi.org/10.1007/s42979-020-00372-z](http://doi.org/10.1007/s42979-020-00372-z)
68. Eappen Geoffrey, Shankar T. Multi-Objective Modified Grey Wolf Optimization Algorithm for Efficient Spectrum Sensing in the Cognitive Radio

Network. *Arabian Journal for Science and Engineering*(2020) [.http://doi.org/10.1007/s13369-020-05084-3](http://doi.org/10.1007/s13369-020-05084-3)

How to cite this article: Eappen G, Shankar T, Nilavalan R. Advanced squirrel algorithm-trained neural network for efficient spectrum sensing in cognitive radio-based air traffic control application. *IET Commun.* 2021;15:1326–1351.
<https://doi.org/10.1049/cmu2.12111>